UNIVERSITY OF CALIFORNIA,
IRVINE

# An Analysis of Recurrent Hippocampal Networks: Synchronization, Time, and Episodic Memory

DISSERTATION

submitted in partial satisfaction of the requirements
for the degree of

DOCTOR OF PHILOSOPHY

in Biomedical Sciences

by

**Conor Dean Cox**

Dissertation Committee:
Professor Gary Lynch, Chair
Professor Christine M. Gall
Professor Richard T. Robertson
Professor Marcelo Wood

2017

# Dedication

To

my friends and family
who helped me become who I am

# Table of contents

# List of Figures

# Acknowledgments

It's difficult to find the words to thank **Dr. Gary Lynch**. By always shooting for the stars, selling projects as the greatest in the world, and never seeing a limit in what I can do, he has pushed me to become better than I could have ever become alone.

I thank **Dr. Christine Gall** for building my work ethic into something I can be proud of with patience, wit, and strict but fair pressure. Also for being an amazing collaborator who was willing to dive into the literature to find an answer, has never hesitated to drive forward and start a new technology or revive an old, and who has pushed our publications to the next level of quality.

The Gall lab and Lynch labs have been my home away from home the last few years. Their members have made the science easier and far better. **Dr. Julie Lauterborn** has been my contact to solve every problem: work, science, or coworkers she always had a solution. It has made life in lab so much more pleasant. A special thanks to **Dr. Christopher Rex** and **Dr. Lulu Chen** I always felt like I was directly walking in your intellectual footsteps and building on the stories you built. **Dr. Yousheng Jia** and **Dr. Ben Gunn** have been fantastic collaborators who have pushed me to learn techniques I would have never tried. Thanks to **Dr. Brittney Cox, Dr. Svetlana Kantorovich, Dr. Ronald Seese**, **Dr. Alex Babayan,** and **Dr. Linda Palmer** for being amazing collaborators, mentors, and friends. **Dr. Carley Karsten**, **Kyle Ellefsen, Kathleen Wang, Aliza Le**, **Danielle Pham, Brian Trieu** and **Lida Agazadah** kept lab and life outside it a little more fun. Thanks also to **Dr. Eniko Kramar, Matiar Jafari, Jihua Liu, Lucy Yao, Bowen Hou**, and **Jeff Rice.**

Thanks to all my collaborators, mentors, teachers, and students who are too numerous to list but specific thanks to **Dr. Shannon Ferris, Dr. Oswald Stewart, Dr. Don Wei, Dr. Danielle Piomelli, Dr. Tallie Z. Baram,** and **Dr. Yuncai Chen** for bringing me in on such exciting and stimulating projects, two of which have dramatically shaped my future directions. Thanks to my committee members **Dr. Marcelo Wood** and **Dr. Richard T. Robertson**. Also to **Steve Tucker, Dr. Matt Grevig,** and **Dr. Neal Woodbury** for setting me on the right direction before and during graduate school.

My undergrads and high school students have pushed me to be a better mentor and have greatly contributed to my work. Especially **Samantha Corwin** and **Leanne Young** who both helped me push stuck projects forward. Also thanks **Sheila Nikdel, Lauren Rameriz, Chelsey Letko, Shiela Shaikh, Loree Karkodorian, Andrew Nguyen, Tiffany Zhang**, **Sophia Byun, Olivia Kim,** and **Alexis Chirco.**

Thanks to my friends outside lab especially **Dr. Anne** who has helped me remain sane throughout my grad career and **Diane** who has kept me mostly healthy despite my best attempts. Also, thanks to **Josh, Nora, Laura, Eric, James, Matt, Dan,** and **Adam.**

None of this would be possible without the billions or even trillions of dollars in free resources available at our finger tips. Thanks to all tool makers, software makers, researchers, tutorial makers, and silent maintainers out there who make this world of science move so rapidly and smoothly. Thanks to the funding from the government and private institutions and the taxpayers who make this whole thing possible, in particular the NIH, ONR, CART, and NSF GRFP.

Finally, thanks to my family. None of this would have begun to be possible without you. Especially thanks to my parents **Douglas** and **Yvonne Cox** for letting me follow my passion into science no matter how much it stole all the magic thinking from the world. Thanks to my sister **Rasma** for always pushing forward. Thanks to my sisters and brothers **Anicca, Claire,** and **Nate** for making Albuquerque even more of a home. Finally to my extended family **Judy, Briana, Bernida, Tom, my grandparents,** and all the others thanks being a part of my life.

Chapter 3 contains material adapted from: Gunn*, B. G., Cox*, C. D. Chen, Y., Frotscher, M., Gall, C. M., Baram, T. Z. & Lynch, G. (4/28/2017) The Endogenous Stress Hormone CRH Modulates Excitatory Transmission and Network. Cerebral Cortex, 1–17.

Chapter 4 contains material from: Cox, C. D., Rex, C. S., Palmer, L. C., Babayan, A. H., Pham, D. T., Corwin, S. D., Trieu, B. H., Gall, C. M., & Lynch, G. (2014). A map of LTP-related synaptic changes in dorsal hippocampus following unsupervised learning. The Journal of Neuroscience : The Official Journal of the Society for Neuroscience, 34(8), 3033–41.

This work was supported by Office of Naval Research Grant N00014-10-1-007, National Science Foundation Grants #1146708, CART, NSF GRFP DGE-0808392, and National Institutes of Health Grant NS045260.

# Curriculum Vitae

**Conor D. Cox**
Cell: (505) 977-531
Email: conorc@uci.edu

3226 GNRF
Irvine, California 92617

## Education

**Ph.D. In Anatomy and Neurobiology** **2010-May 2017**
*University of California, Irvine*
Doctoral Adviser: Gary Lynch Ph.D.
"Emergence of episodic memory from hippocampal CA3"

**BS In Biochemistry** **2006-2010**
*Arizona State University, Tempe, AZ*
Adviser: Neil Woodbury Ph.D.
"High-throughput screening in two dimensions: Binding intensity and off-rate on a peptide microarray"

**Additional Coursework**
New England Complexity Sciences Institute: "Complex Physical, Biological and Social Systems" and "Building Models and Mapping Networks" 2016.
Coursera: Computational Photography and Machine Learning 2013.
UCI Training: Introduction To Linear And Logistic Regression Models For Medical Researchers 2013, 2014. Introduction to High Performance Computing- 2015. Geometric Optics 2016.

## Honors

NSF Graduate Research Fellowship 2012-2015
Top Presentation Anatomy And Neurobiology Grad Day 2015
National Merit Scholarship 2006-2010
Biochemistry BS Award 2010
Dean's Circle Scholarship 2009
CRC Handbook of Chemistry and Physics Outstanding 1st Year Award 2006

## Publications

Gunn*, B. G., **Cox***, **C. D.** Chen, Y., Frotscher, M., Gall, C. M., Baram, T. Z. & Lynch, G. (2017) The Endogenous Stress Hormone CRH Modulates Excitatory Transmission and Network. *Cerebral Cortex*, 1–17

**Cox, C. D.**, Rex, C. S., Palmer, L. C., Babayan, A. H., Pham, D. T., Corwin, S. D., Trieu, B. H., Gall, C. M., & Lynch, G. (2014). A map of LTP-related synaptic changes in dorsal hippocampus following unsupervised learning. *The Journal of Neuroscience : The Official Journal of the Society for Neuroscience*, *34*(8), 3033–41.

Wang, W., Jia, Y.  Pham, D.T., Palmer , L.C., Jung, K.M., **Cox, C.D.**, Rumbaugh, G,. Piomelli, D., Gall, C.M., Lynch, G., (2017) Atypical Endocannabinoid Signaling Initiates a New Form of Memory-Related Plasticity at a Cortical input to Hippocampus. *Cerebral Cortex*, 1–14

Lauterborn, J. C., Kramár, E. A., Rice, J. D., Babayan, A. H., **Cox, C. D.**, Karsten, C. A., Gall, C. M., & Lynch, G. (2016). Cofilin Activation Is Temporally Associated with the Cessation of Growth in the Developing Hippocampus. *Cerebral Cortex (New York, N.Y. : 1991)*, bhw088

Lauterborn, J. C., Palmer, L. C., Jia, Y., Pham, D. T., Hou, B., Wang, W., Trieu, B. H., **Cox, C. D**., Kantorovich, S., Gall, C. M., & Lynch, G. (2016). Chronic Ampakine Treatments Stimulate Dendritic Growth and Promote Learning in Middle-Aged Rats. *The Journal of Neuroscience : The Official Journal of the Society for Neuroscience*, *36*(5), 1636–46.

Wei, D., Lee, D., **Cox, C. D.**, Karsten, C. A., Peñagarikano, O., Geschwind, D. H., Gall, C. M., & Piomelli, D. (2015). Endocannabinoid signaling mediates oxytocin-driven social reward. *Proceedings of the National Academy of Sciences of the United States of America*, *112*(45), 14084–9.

Trieu, B. H., Kramár, E. A., **Cox, C. D**., Jia, Y., Wang, W., Gall, C. M., & Lynch, G. (2015). Pronounced differences in signal processing and synaptic plasticity between piriform-hippocampal network stages: a prominent role for adenosine. *The Journal of Physiology*, *593*(13), 2889–2907.

Lynch, G., **Cox, C. D**., & Gall, C. M. (2014). Pharmacological enhancement of memory or cognition in normal subjects. *Frontiers in Systems Neuroscience*, *8*(May), 90.

Farris, S., Lewandowski, G., **Cox, C. D.,** & Steward, O. (2014). Selective localization of arc mRNA in dendrites involves activity- and translation-dependent mRNA degradation. *The Journal of Neuroscience : The Official Journal of the Society for Neuroscience*, *34*(13), 4481–93.

Seese, R. R., Chen, L. Y., **Cox, C. D**., Schulz, D., Babayan, A. H., Bunney, W. E., Henn, F. A., Gall, C. M., & Lynch, G. (2013). Synaptic abnormalities in the infralimbic cortex of a model of congenital depression. *The Journal of Neuroscience : The Official Journal of the Society for Neuroscience*, *33*(33), 13441–8.

Seese, R. R., Babayan, A. H., Katz, A. M., **Cox, C. D.**, Lauterborn, J. C., Lynch, G., & Gall, C. M. (2012). LTP Induction Translocates Cortactin at Distant Synapses in Wild-Type But Not Fmr1 Knock-Out Mice. *Journal of Neuroscience*, *32*(21), 7403–7413.

Kramár, E. A., Babayan, A. H., Gavin, C. F., **Cox, C. D.**, Jafari, M., Gall, C. M., Rumbaugh, G., & Lynch, G. (2012). Synaptic evidence for the efficacy of spaced learning. *Proceedings of the National Academy of Sciences of the United States of America*, *109*(13), 5121–6.

Greving, M. P., Belcher, P. E., **Cox, C. D.**, Daniel, D., Diehnelt, C. W., & Woodbury, N. W. (2010). High-throughput screening in two dimensions: Binding intensity and off-rate on a peptide microarray. *Analytical Biochemistry*, *402*(1), 93–95.

## In review

**Cox, C.D.*,** Palmer, L.C.*, Pham, D.T., Trieu, B.H., Gall, C.M., & Lynch, G. (2017) Transfer of Experiential Learning in Rodents: Past Experience Enables Rapid Learning and Localized Encoding in Hippocampus. *Submitted. Learning and Memory*

Wang, W, Cox, B.M., Jia Y., Le, A.A., **Cox, C.D.**, Jung, K.M., Hou, B., Piomelli, D., Gall, C.M. & Lynch, G. Treating a novel plasticity defect rescues episodic memory in Fragile X model mice. *Submitted. Molecular Psychiatry*

## Mentorship

**Undergraduates Mentored:**
Samantha Corwin, Sheila Nikdel, Lauren Rameriz. Chelsey Letko, Shiela Shaikh, Loree Karkodorian, Andrew Nguyen, Leeanne Young
**High School Students Mentored:**
Tiffany Zhang, Sophia Byun, Olivia Kim, Alexis Chirco
**Student Recognition:**
Sheila Nikdel- Undergraduate Excellence
Samantha Corwin- Summer Undergraduate Research Program Funding
Olivia Kim and Alexis Chirco-1st Prize Cognitive Sciences Orange County Science Fair
**Outreach:**
Tech Trek (lab tour for middle school students) 2013-2014
Moderator and founding member of reddit.com/r/askscience (A forum for general audience to ask science questions with 13m users) 2010-present
**Open source contribution:**
Two models submitted for public access to ModelDB

## Teaching

Lead instructor: UCI Neuroscience Programming Club 2013-2015
Teaching assistant: Human Development: Conception to Birth 2012

## Selected Presentations

**C. D. Cox** (2017) “The epileptogenic hippocampal CA3: contributions to serial learning” *Epicenter* (Invited)

B. G. Gunn, **C. D. Cox**, Y. Chen, C. M. Gall, G. Lynch, T. Z. Baram; (2016) Endogenous CRH enhances excitatory synaptic transmission and intrinsic hippocampal network activity. *Society for Neuroscience*

J. C. Lauterborn, L. C. Palmer, Y. Jia, B. Hou, D. T. Pham, W. Wang, B. H. Trieu, **C. D. Cox**, S. Kantorovich, C. M. Gall, G. Lynch; (2015) Ampakines stimulate dendritic growth in the hippocampus of middle-aged, environmentally enriched rats. *Society for Neuroscience*

B. H. Trieu, E. A. Kramar, Y. Jia, W. Wang, **C. D. Cox**, D. T. Pham, C. M. Gall1, G. Lynch; (2014) Processing of theta input differs markedly at the individual stages of the piriform-hippocampal network. *Society for Neuroscience*

A. Vogel-Ciernia, D. P. Matheos, E. Kramar, B. Trieu, **C. Cox**, C. Magnan, M. Zeller, A. Tran, A. Lopez, K. Sakata, S. Azzawi, R. Dang, R. Barrett, P. Baldi, G. Lynch, M. Wood (2014) Subdomain 2 of the neuron-specific chromatin remodeling subunit BAF53b is required for synaptic plasticity and memory *Society for Neuroscience*

C. A. Karsten, **C. D. Cox**, K. Wang, G. Lynch, C. M. Gall (2014) Differences in network activation patterns may underlie learning enhancement with spaced training *Society for Neuroscience*

**C. Cox**, A. H. Babayan, L. C. Palmer, C. S. Rex, D. T. Pham, B. Trieu, C. M. Gall, G. Lynch; (2012) Regionally differentiated synaptic modifications with learning in adult rat hippocampus. *Society for Neuroscience*

M. Jafari, A. H. Babayan, J. C. Lauterborn, **C. D. Cox**, C. M. Gall, G. Lynch (2011) Spine distribution of increases in F-actin with induction of LTP. *Society for Neuroscience*

## Skills

Python (numpy, scipy, scikit-image), Computational Neuroscience, Microscopy (Confocal, Epifluorescence, Two Photon), behavioral analysis, Immunohistochemistry, Network Analysis, Complexity, Agent Based Modelling, UNIX, High Performance Cluster Computing, Machine Learning, Computational Imaging, Microscopy Design, Geometric Optics, Statistics, Matlab, R, ImageJ, Digital Signal Processing, Photoshop, Illustrator, Inkscape. Neural Networks, OpenCV, Computer Vision, Statistical Analysis, Prism, Factor Analysis, Clustering, Markov Models

# Abstract of the Dissertation

An Analysis of Recurrent Hippocampal Networks: Synchronization, Time, and Episodic Memory

By

Conor Dean Cox

Doctor of Philosophy in Biomedical Sciences

University of California, Irvine, 2017

Professor Gary Lynch, Chair

Episodic memory is the memory of complex sequences of events; basically memories that contain information about 'what' occurred, 'where' it happened, and 'when'. It is unclear how episodic memory is stored in the brain. The first part of this dissertation presents a model whereby the recurrent connections of hippocampal field CA3 are used to store a cue while tracking its appearance in time to allow the trace of temporally separated cues to be bound by long term potentiation (LTP). This process allows disparate elements of an episode to be linked and recovered in correct order while maintaining their temporal relationships. The proposed activities of field CA3 evident in the model were then validated by electrophysiological experiments showing that the CA3 network can produce long and broad network reverberations in vitro without the reverberation of individual pyramidal cells. Additional studies demonstrated that CA3 was required for storage of the 'when' component of episodic memory.

Episodic memory storage and organization happens continuously without supervision; however animals and humans use past experience to organize incoming complex information. Research described in the second part of the dissertation used exploration and learning of a complex unsupervised environment to test if prior experience with environmental complexity influenced exploration strategies and learning. We found that rats spontaneously organize their

behavior into episodes and that rats with prior experience with complexity use these episodes to more efficiently explore and learn the environment as compared to rats with prior exercise or handling. Using this behavioral task we then determined where learning-related synaptic modifications occurred. Analysis of the distribution of synapses with evidence of recent LTP showed that 'prior experience' animals store their information in spatially discrete segments of hippocampus, and primarily in field CA1. We then used a second behavioral task to determine where episodic vs contingency-based learning was stored. We found that in the exploration paradigm, synaptic changes associated with exploration were prominent in a different collection of zones including CA1 striatum oriens and CA3c. These mapping studies reinforce the conclusion that different types or components of memory are encoded through activities of different hippocampal subfields.

# Introduction and Overview of the Dissertation

Episodic or narrative memory involves the assembly of a complex sequence of disparate types of information into a unit (Tulving, 1985). Such episodes contain truly remarkable amounts of data about the nature of dozens of cues ('what'), their spatial relationships ('where'), and the temporal order and delays between them ('when') (Clayton et al., 1998). These points help explain the immense capacity of memory and the ability to quickly retrieve particular items, a process that commonly involves locating an episode and then searching through it for the target items. Despite considerable evidence that these activities are central to cognition and inferential thinking, little is known about how they are executed by brain networks. The first part of this dissertation addresses an important part of this question: how elements are linked together during experience and then recalled in a proper sequence. An hypothesis will be evaluated in which the remarkable recurrent collateral system found in hippocampal field CA3 allows for recurrent activation of neurons, thereby maintaining a representation of a cue long past the period in which it was actually present. This 'trace' can then be linked to a later arriving input via conventional mechanisms of long term potentiation (LTP). Arguments postulating that interconnected neurons can provide a kind of transient memory have a long history in neuroscience and the proposed role for CA3 is a logical extension of this. (Amit, 1995; Compte et al., 2000; Hopfield, 1982; Marr, 1971) Relatedly, there is a growing consensus that an essential function of the hippocampus involves temporal processing of a type beyond the capabilities of the much more elaborate circuitry found in cerebral cortex.(Eichenbaum, 2014) The commissural/associational system of field CA3 has no parallels, regarding the presence of massive reverberating associational connections, elsewhere in the extended hippocampal formation or in the telencephalon and thus is a logical site for the execution of the postulated time related functions of hippocampus.

Assuming, as is the case here, that most complex computations by brain represent network level operations, then simulations of large numbers of neurons provide the only currently available means for investigating the proposed role of CA3. We therefore built a biophysical model with more than one thousand neurons along with anatomically dictated connections, interneurons, and inputs from the dentate gyrus and entorhinal cortex to determine if the basic design of CA3 is capable of the above across time operations. Simulations of this type serve to define minimal sufficient conditions for performing the suspected function (association between delayed cues) but are also useful for identifying unsuspected neurobiological features required for the function. Because of their considerable complexity, and incorporation of stochastic features of neurons, simulations on occasion generate unexpected effects that are of computational and psychological interest. They also allow direct manipulation of parameters in order to gain insight into to how, and under what conditions, the anatomically- and physiologically-based model produces such effects, and by extension how these behaviors may be possible in biological neuronal networks. As will be described, the present model produces effects that go well beyond cue linkages and that are key features of episodic memory.

We supplemented the modeling work with experiments to test specific predictions of the hypothesis that the dense associativity of the CA3 system enables the temporal functions of the hippocampus in laying down an episodic memory trace. Surprisingly, there have previously been no direct tests of the common assumption that reverberating activity maintained by the recurrent collateral projections can maintain firing by individual pyramidal neurons. The simulations also suggested a first direct test of the central argument that field CA3 is essential for encoding the temporal order in which cues occur. This project required the development of novel rodent behavioral paradigms for assessing the basic ‘what’, where’, and ‘when’ elements of an episode.

Organizing the flow of experience into discrete episodes occurs continuously and without supervision. It is undoubtedly the case, however, that people use their past experience with complex environments to guide the acquisition of now present episodic information. This process of transferring rules or strategies from earlier encounters with the real world is a prominent topic in human research (Baldwin et al., 1988; Pan et al., 2010). It follows from these points that analysis of episodic like memory in animals will ultimately have to employ behavioral paradigms involving unsupervised movement through environments containing ‘what’, ‘where’, and ‘when’ data as well as subjects with a history of dealing with complexity. As described below, we have gradually evolved a first protocol that incorporates these features and in which rats use discrete, episode-like forays to explore a novel, challenging environment. These developments allowed us to identify the nature of the material transferred from prior encounters with complexity and to show that this process markedly enhances memory formation, advances that bring the animal work substantially closer to the human condition.

Using the above behavioral tests, we addressed the question of where learning related synaptic modifications occur in the hippocampus when animals are using multiple episodes to master complex, high choice situations. The results were unexpected and suggest that an integration of experience, rather than acquisition of specific information, dominates hippocampal encoding in realistic real world conditions.

# Chapter 1 Recurrent Networks as a Means for Associating Temporally Spaced Cues

Connecting cues separated in time is a fundamental memory operation but one that presents serious, largely unrecognized problems for current neurobiological and computational hypotheses about synaptic encoding operations. (Wallenstein et al., 1998) It is broadly assumed that memory-related synaptic modifications occur when an afferent input and its target neuron are activated at the same time. This hypothesis, often referred to as the 'Hebb Rule', proves to have powerful computational advantages, as shown in hundreds of network models (Bienenstock et al., 1982; Hopfield, 1982). The discovery and subsequent analysis of long-term potentiation (LTP) described a biological implementation for the above simple version of the rule (Bliss et al., 1993) (other aspects of the postulated Hebb synapse are not realistic) (Granger et al., 1994). LTP is an activity-induced increase in synaptic strength. The LTP effect occurs when the presynaptic depolarization and release is accompanied by the engagement of voltage sensitive postsynaptic receptors, something that requires an unusual level of postsynaptic depolarization. Thus, pre- and post-synaptic events must occur within a narrow time frame as proposed in the Hebb rule. LTP satisfies demanding constraints for a memory mechanism: it is induced by naturalistic patterns of afferent activity, occurs in a synapse-specific manner, and can last for weeks or longer (Abraham et al., 2002; Baudry et al., 2011; Lynch et al., 1984). However, the very requirement for temporal contiguity raises the problem of how *two cues spaced in time by hundreds of milliseconds or more become associated by LTP-type plasticity*. This problem has received surprisingly little attention from neuroscientists and persons modeling neuronal networks but one of two solutions is usually advanced when the issue does arise: 'fire and hold' cells of the type found in motor systems, and reverberating network activity (Eichenbaum, 2014; Jochems et al., 2013; Wallenstein et al., 1998). The hippocampus plays a critical role in the learning of sequential cues and thus it is a logical site to test for these two

mechanisms (Dede et al., 2016; Farovik et al., 2010). This chapter first describes the anatomy of hippocampus and then considers the possibility that recurrent networks in the structure could provide the substrate for linking temporally displaced cues.

**1-1. Hippocampal anatomy and cue association.**

The hippocampus receives its primary input from entorhinal cortex (ERC), a complex area itself, receives input from diverse set of regions (Oh et al., 2014; Seltzer et al., 1976). In network maps of the brain, it often emerges as a central hub of convergence of lower level sensory networks and higher-level memory and processing network. And, in a recent analysis of connectivity among cortical regions, the lateral aspect of ERC stood out as the cortical field with connections to the greatest number of cortical regions (Bota et al., 2015). The ERC also contains a clearly delimited topography along several axes. The medial portion of the entorhinal cortex (MEC) has been proposed as a major site of convergence of sensory information relating to an animal's location in space and contains cells that help map location in extended environments (Hafting et al., 2005; Hargreaves et al., 2005). This is also the likely relay for transmitting auditory cues to the hippocampus (Chen et al., 2013; Deadwyler et al., 1979). The lateral portion of entorhinal cortex (LEC) is primarily concerned with cue identity(Eichenbaum et al., 2012; Wilson et al., 2013). The neurons within layer 2 of both the medial and lateral entorhinal cortices project to the dentate gyrus, which is the primary site of information transfer into hippocampus (Rolls, 2008). This projection has an interesting topography, the LEC projects to the distal one third of the dendritic layer of the dentate gyrus (the dentate gyrus molecular layer) while the MEC innervates the middle third (Amaral et al., 2007). Both collections of ERC fibers continue into pyramidal cell field CA3, which also receives processed and heavily filtered information from the dentate gyrus via the peculiar mossy fiber axons of the dentate gyrus granule cells. Layer 3 cells of LEC also connect to pyramidal neurons of field CA1 (Treves et al., 1994). These projections are to the most distal portion of target dendrites and are thought to require repeated spiking or coordinated input from CA3 to bring CA1 neurons to their firing

threshold (Jarsky et al., 2005). Layer 5 cells in the ERC receive input (and, in a sense circuit feed-back input) from the CA1 and subicular pyramidal cells. This deep layer projects to the more superficial layers of ERC resulting in a many stage entorhinal-hippocampal-entorhinal loop (Canto et al., 2008); in vivo physiological recording studies have confirmed that this system can support the transmission of a signal from the hippocampus to the ERC and then back to hippocampus (Deadwyler et al., 1976).

The hippocampus on the other hand has a heavily structured topography. It has three evident subdivisions (dentate gyrus, CA3, CA1) recognized by early anatomists to constitute a serial network that later workers sometimes refer to as the 'tri-synaptic circuit'. As mentioned above, the entorhinal cortex densely innervates the two outer lamina of the dentate gyrus; the inner dendritic zone receives a topographically dispersed excitatory input from the cells located below the primary neurons (granule cells) of the dentate gyrus (Deadwyler et al., 1975). These neurons are targets of granule cell axons, resulting in a positive feedback loop. Interestingly, the three major, laminated afferents to the granule cell dendrites each express a different version of LTP (W. Wang et al., 2016). If and how these elements interact to bind the object and space information transmitted from the entorhinal cortex is a matter of active research. The dentate gyrus granule cells generate the mossy fiber axons that project in a tight bundle to the most proximal dendrites of the CA3 pyramidal cells. This is one of the most unusual connections in the brain. It is extremely sparse with each fiber connecting to approximately 15 cells and each CA3 neuron only receiving input from 50 granule cells (Amaral et al., 1990; Treves et al., 1994). However, the projection is also extremely potent: mossy fiber boutons envelope multiple spines near the soma of CA3 cells leading to 'detonator' synapses (Urban et al., 2001).

Field CA3 is the second stage of hippocampal processing and, like the dentate, is an unusual structure. Its pyramidal cells receive ~70% of their input from within CA3, and specifically from pyramidal cells of CA1 (Amaral et al., 1990; Treves et al., 1994), with about half of this coming from the contralateral side; this massive commissural/associational system is a

singular feature of hippocampus. Because of this, the region has been the subject of a number of modeling studies with the major hypothesis being that CA3 is the primary site of object identity storage (Kesner et al., 2015). This is due to its superficial similarity to the proposed Hebb-Marr nets (Marr, 1971), which were later adapted into Hopfield nets (Hopfield, 1982), a computational model that is capable of storing inputs, retrieving degraded information, and recovering sequences with no gaps. Work of this type led to the broad idea that CA3 constitutes a 'pattern completion' system, though it's operation as a Hebb-Marr net would require features that are not known for field CA3 (for example, the capacity to erase stored information) (Dunwiddie et al., 1978; Kesner et al., 2015).

The third and final stage of the hippocampal network is field CA1, a region that is anatomically relatively simple in comparison to the CA3 and DG. It receives inputs topographically from field CA3 with those cells closer to the DG (CA3c) projecting to the more distal portions of the CA1 dendrites, and those closer to the CA1 terminating more proximally on the CA1 dendritic tree. CA3 neurons located closest to CA1 project the basal side of the target dendritic tree, a region that is unusually responsive to synaptic modification. (Roth et al., 1995) Interestingly, no matter where the input is along the CA1 dendrite, it's response at the cell body is relatively constant. Synapses further from the cell body have been shown through multiple means to have more receptors than those terminating more proximally such that similar physiological responses occur along the whole dendritic tree (Jarsky et al., 2005; Nicholson et al., 2006; Smith et al., 2003). This feature of CA1 is not found elsewhere in the cortex.

Two sites in the above architecture have been proposed to implement the above noted mechanisms for linking cues separated in time. Regarding the idea that individual neurons serve this role, results from chronic recordings suggest that layer 2 cells in the MEC contribute to encoding of cue sequences by hippocampus via repeated firing in gap-times between cues. However, this effect could be secondary to prolonged events in the hippocampus that are fed back to the MEC via CA1 and subiculum; there is also a possibility that the animal maintains

contact with a first cue before shifting its attention to a later one (Jochems et al., 2013). Other work has used a pharmacological treatment to test if layer II entorhinal neurons express the 'fire and hold' property that could serve to link separated stimuli (Hasselmo et al., 2006). In one study, twenty percent of the cells were found to continue spiking in vitro and in vivo after activation in the presence of carbachol, a cholinergic receptor agonist that depolarizes neurons and thereby brings them closer to the action potential threshold (Jochems et al., 2013). While of considerable interest, these results do not document the presence of fire and hold neurons, as described for striatum, in hippocampal networks. However, some theorists have built on the data for such specialized neurons to develop a hypothesis in which the direct connections from ERC to field CA1 constitute a system for associating cues across time without the rest of the hippocampus (Jochems et al., 2013). This proposal makes fairly few network predictions as it is strictly biophysical and raises a number of largely ignored problems, such as how these cells are turned off, and what determines which of them fire and hold vs. fire and forget. It would in any event be surprising if the relatively weak entorhinal input to CA1 were solely responsible for what is thought to be a fundamental hippocampal operation.

The second postulated mechanism for maintaining signals so as to allow for associations across time --- sustained firing due to dense interconnectivity between neurons --- aligns with the above-summarized anatomy of field CA3 (Wallenstein et al., 1998). And brain slice experiments show that the region occasionally (1-3 times per second) and spontaneously synchronizes its neurons, creating large extracellular potentials referred to as Sharp Waves (SPW). These events had been known for years from chronic recording studies of animals but their comparable occurrence in slices strongly encourages the idea that even relatively small populations of CA3 neurons periodically engage in sustained firing due to recurrent networks (Rex, Colgin, et al., 2009). However, experimental or modeling evidence for the idea is lacking.

Testing for sustained activity via recurrent connections is difficult. It necessarily involves large numbers of CA3 cells, likely separated by considerable distances to account for the time

delays necessary to allow for maintenance of a signal. It is important to note that in these regards sustaining a representation of a transient cue does not necessarily imply that the same neurons are held in an active state until the arrival of a second cue. Given a sufficiently dense associative network, stimulation of an original population of cells could result in a series of active cell populations that cycle among themselves for extended periods of time. In this sense, associations between cues would involve an association between derivatives of the original representation active at the time delay in which the second signal arrived. Testing such ideas even with very large numbers of recording electrodes or with calcium imaging is not feasible because of distances involved and the possibility, noted above, that the pertinent cell populations are continually evolving. The alternative is to generate biologically grounded models that allow for predictions of what might be required for a network to generate these operations.

The following section develops and modifies a biophysical model of SPWs generated by CA3 to include a dentate gyrus input. It then tests the traits of this model to determine the range of potential outputs and then moves to the question of whether modified versions of the simulation support sustained firing of neurons over psychologically meaningful time scales. Initial tests for such activity in brain slices are also described. We then ask if the addition of an LTP-effect to the model enables a simple but fundamental behavioral phenomenon involving cue associations across time.

**1-2. Description of the model (adapted from (Gunn et al., 2017)).**

We used SPWs, large composite excitatory post synaptic potentials (EPSPs) that form part of the SPW-ripple complex, as an initial endpoint measure. SPWs originate autonomously within subfield CA3b, in part resulting from stochastic release from mossy fibers, and propagate to the remainder of hippocampus via the dense CA3 associational projections (Kubota et al., 2002; Rex, Colgin, et al., 2009). Moreover, the initiation and characteristics of SPWs are

regulated by GABAergic interneurons and modulatory inputs to the hippocampus (Hajos et al., 2013; Kubota et al., 2002; Maier et al., 2003; Rex, Colgin, et al., 2009; Schlingloff et al., 2014). SPWs are a well-characterized example of the coordinated operation of CA3 cells acting through their unusually dense associational projections (Buzsáki, 1986; Kubota et al., 2002). The initiation of SPWs requires both excitatory and inhibitory transmission, although a consensus on the essential mechanisms remains to be established.

We modified a previously reported CA3-CA1 hippocampal model that produces simulated SPWs (Taxidis et al., 2012) to include a dentate gyrus (DG) component, and used this model to assess the influence that synaptic transmission at the single cell level has upon the generation of these network events. Briefly, the DG was comprised of 1000 cells with no recurrent connections and a low probability (1 in 1000) of connectivity to CA3 pyramidal cells. The DG activity was determined using a Poisson distribution around a set frequency. The CA3 and CA1 were comprised of 1000 pyramidal cells and 100 interneurons each (i.e. 10:1 pyramidal cell to interneuron ratio). The distance between neurons was 10 μm for both regions, with interneurons positioned equidistantly (one every ten cells) throughout the array. Pyramidal cells were modelled by the two-compartment Pinsky-Rinzel model (Pinsky et al., 1994) adapted from ModelDB (accession no 35358; Migliore et al., 2003) while interneurons were modelled on the single-compartment Wang-Buzsaki model (Wang & Buzsáki, 1996). In CA3, pyramidal cells were recurrently connected to each other as well as to inhibitory interneurons, providing strong feedforward and feedback inhibition. In contrast, CA1 interneurons were strongly connected with one another without recurrent excitatory connections. The CA3 and CA1 arrays were separated by a distance of 100 μm, with CA3 pyramidal cells connecting to both pyramidal cells and interneurons within the CA1. A Gaussian distribution was used to determine the probability of connectivity among cell types as previously described (Taxidis et al., 2012). (**Fig. 1-1**). In both the CA3 and CA1, excitatory and inhibitory synaptic interactions among cells were mediated by AMPA and $GABA_A$ receptors respectively. Synaptic interactions were modelled as previously

described where the synaptic conductance was set to 1 nS for all synapses (Taxidis et al., 2012); see supplemental methods). As such, the strength of synaptic events was controlled by the variable $\alpha_{syn}$. Values for $\alpha_{syn}$ were specific for each excitatory and inhibitory synapse among cells**.** The decay time ($\tau$) of excitatory currents was set to 2 ms, and for $GABA_AR$-mediated currents at 7 ms and 2 ms for synapses targeting pyramidal cells and interneurons, respectively. Conductance velocity for pyramidal cell axons (CA3 and CA1) was 0.5 mm/ ms, and for CA1 and CA3 interneurons conductance velocities were set as 0.1 mm/ ms and instantaneous respectively (Taxidis et al., 2012). Heterogeneity in the system was introduced through variation in the reversal potential of neurons that was distributed over cells using a Gaussian distribution. A firing reset voltage of -60 mV was introduced. To prevent oscillations in cell voltages (and model collapse) the maximum number of synaptic inputs to an individual cell, at the same time, was capped at 100.

We used the DG-CA3-CA1 model to examine the effect of changes in the frequency of EPSCs targeting CA3 pyramidal cells on the generation of SPWs in both the CA3 and CA1 arrays. The frequency of simulated EPSCs onto CA3 pyramidal cells was sensitive to 1) the frequency of DG activity and 2) the strength of excitatory synaptic conductance (scaled DG and CA3 synapses). Frequency of DG activity was increased at 0.5 Hz increments (range 0.5 to 4 Hz) and the frequency of EPSCs in CA3 pyramidal cells and the number of SPWs in CA3 and CA1 were quantified. The synaptic strength onto CA3 pyramidal cells was similarly increased in 0.5 increments (arbitrary units [a.u.] in range 0.5 to 3.5) and frequencies of EPSCs and SPWs similarly assessed. The hippocampal model was run over a 10 second period and repeated 10 times for each DG frequency and synaptic strength value.

The effect that the residual depolarizing current onto CA3 pyramidal cells had upon generation of SPWs in CA3 and CA1 was assessed using the adapted CA3-CA1 model (i.e. without a DG component). A depolarizing current was applied to CA3 pyramidal cells for the duration of each simulation (i.e. 10 seconds), with a range in amplitude of 0.15 to 0.24 nA, and

the frequency of SPWs in the CA3 and CA1 arrays were measured. This model was run over a 10 second period and repeated 10 times for each different current step.

The effect that synchronization of multiple mossy fiber inputs had upon SPW generation in the CA3 array was assessed by determining how the number of DGGC cells firing (% of total) over different periods of time (10, 50, 100 and 200 ms) influenced the probability of a single SPW occurring. We identified a threshold that seemed to be of physiological relevance, in this case 200 DGGCs (i.e. 20 % of total), and the probability of a SPW being generated was calculated from a 1 second period that was repeated 30 times for each time period (i.e. 10, 50, 100 and 200 ms). We used a synaptic strength measure of 1.5 a.u. for our baseline measure that was reduced to 1.4 a.u. to model potential effects of CRHR1 inhibition.

A SPW was defined as >100 cells firing within a 50 ms time period in the CA3 array and >500 cells firing within the same time epoch in CA1. Adjacent epochs that were also above threshold were considered the same event. The frequency of SPWs was calculated as the number of events over the 10 second run time. SPW traces were generated from 55 firing cells, consisting of both pyramidal cells and interneurons, and were displayed as the average $V_{membrane}$ across these cells. The potential difference (i.e. $V_{membrane}$) was recorded from the dendritic and somatic compartment of pyramidal cells and interneurons respectively. A similar approach was used to generate the firing properties of individual CA1 pyramidal cell and interneuron firing patterns during a SPW.

The frequency of EPSCs was determined using an amplitude threshold (-5 mV) with a baseline reset of -2 mV. The hippocampal model was run over a 10 second period and repeated 10 times for each DG frequency and synaptic strength. SPW frequency was calculated from the number of events per 10-second simulation run.

**1-3. The simulation spontaneously generates sharp waves.**

Recurrent connections between CA3 neurons resulted in widely spaced synchronization of spontaneous EPSCs measured in CA3 neurons, as occurs during SPWs (**Fig. 1-2a**). These composite events were spaced apart by hundreds of milliseconds and in this regard resembled the extracellular waves recorded in slices (**Fig 1-2b**). The level of depolarization produced was substantially greater than the amplitude of evoked EPSCs routinely recorded as fEPSPs; thus, the SPWs seen in the simulation would be readily detected with extracellular electrodes. We investigated the nature of pyramidal cell and interneuron spiking (at the single neuron level) related to population level behavior of the network. The simulated firing rate was higher in CA1 pyramidal cells and interneurons in comparison to their CA3 counterparts, most likely due to amplification of CA3 output, associated with a high level of connectivity between CA3 pyramidal cells and CA1 neurons. Consistent with experimental data (Rex, Colgin, et al., 2009), the strength of mossy fiber synapses (i.e. $\alpha_{syn}$, see above) within our simulation greatly influenced the generation of SPWs. Furthermore, the degree of synchronization of a threshold level of mossy fiber input (20 % of DGGC firing) was found to profoundly influence the probability of SPW initiation. Specifically, 20 % of DGGCs firing over a 10, 50, 100 and 200 ms period resulted in a 23 %, 7 %, 3 % and 0 % chance of a SPW occurring within the CA3, respectively.

We tested if a change in the frequency of excitatory synaptic transmission influences SPW generation in the hippocampal simulation. Because the model has no cortical inputs (i.e. no input from entorhinal cortex), we modulated the frequency of EPSCs onto CA3 pyramidal cells by manipulating the nature of the output from the DG. Increasing the frequency of DG output resulted in an activity-dependent increase in the frequency of EPSCs in individual CA3 pyramidal cells (**Fig 1-2c,d**). Remarkably, this effect was associated with a greater incidence of SPWs in both CA3 and CA1 (**Fig 1-3c,d**). Thus, the model faithfully recapitulated electrophysiological observations using antagonists of small endogenous peptides (Gunn et al., 2017). Additionally, increasing the frequency of EPSCs on to CA3 pyramidal neurons via a

second manipulation (enhancing the scaled synaptic strength; **Figure 1-3a,b**), also resulted in augmented SPW frequency in both regions. (This effect was likely associated with a reduction in the probability of SPW generation as reducing the scaled synaptic strength (from 1.5 to 1.4 a.u.) completely attenuated the likelihood of SPW initiation at threshold levels (20 % DGGCs firing) and was irrespective of input synchrony to CA3 pyramidal cells.

To probe if augmentation of SPW generation was specifically associated with phasic excitatory transmission, we used the hippocampal model to examine how the amplitude of a residual excitatory current in CA3 pyramidal cells influenced these events. Interestingly, increasing the amplitude of such a depolarizing current in CA3 pyramidal cells had no effect upon the frequency of SPWs in the CA3 (**Fig 1-4a,d**), but did cause a reduction in the amplitude of these events (**Fig 1-3a bottom**). The reduced amplitude and lack of effect upon the frequency of SPWs in the CA3 array likely results from a desynchronization of pyramidal cell spiking as illustrated by the raster plot (**Figure 1-5A top**) and the observation that the size of pyramidal cell clusters does not change in response to the residual current amplitude (**Fig 1-3b$_1$**). However, the number of pyramidal cell clusters does increase in an input-dependent manner (**Fig 1-3b$_2$**) and may explain the qualitative increase in the small SPW-like events observed in the CA3 (**Figure 1-3a bottom**). Paradoxically, increasing the residual excitatory current in CA3 pyramidal cells did result in an increase in the SPW frequency in the CA1 (**Fig 1-5B, D**). This effect likely results from the strong amplification of the signal generated by the small clusters of pyramidal cells spiking in CA3 (**Figure 1-3a**) through the Schaeffer collateral connection to the CA1 array (**Fig 1-1**).

In all, the model faithfully generates the emergent, and network synchronizing SWRs, recapitulates several physiologically realistic phenomena previously predicted and seen in vivo, and generates surprising behavior, the cell clustering from current input, that hints at a potential difference between what is seen with dentate stimulation, and what is seen by direct current injection, as might be seen during theta. Primarily, increasing the strength or frequency of the

strength of the dentate input directly leads to increases in the out rate of sharp wave ripples, an unsurprising result given that both lead to a type of convergence on a small number of inputs. Also, as the machinery in the CA3 was necessary to generate SPWs, this implies, if episodic information is contained within them, as has been postulated my many labs, that episodic information cannot be primarily contained in the CA1 as required by the 'fire and hold' literature. The heterogeneous output of this model and its biological accuracy make it a tantalizing target for further investigation of the CA3 recurrent connections and their role in memory. To this end the model will be simplified for speed and LTP will be added to produce tight cores of converging activation, which emerge spontaneously in this model.

**1-4. Associating temporally separated cues.**

Changes to the model. We added LTP to the simulation as an increment of baseline (excitatory) synaptic strength for a collection of active inputs that produced a large increase in postsynaptic calcium. These are conditions in which stable potentiation occurs in slices and in vivo. LTP was not included in the mossy fibers in our first tests. Other changes to the system included the following: the neurons were simplified from Pinksy-Rinzel cells to Wang-Buszaki cells. As the primary feature needed from these neurons was their ability to feed signal and not their specific biophysical characteristics, Pinksy-Rinzel cells run approximately 2-3x slower in simulation so the neurons were simplified to allow for more rapid prototyping. Second, CA3 cells were resorted to allow interconnected subnetworks to be spatially close. (**Fig 1-6B)** In the real CA3 network, recent papers, and the model presented below, predict that recurrent networks in the CA3 will be broadly spatially spread to allow multiple input delays. Physiological evidence presented later will provide a potential mechanism for this spreading. However, this would require a massive network, which would be incompatible with simulation and even less compatible with rapid prototyping. To fix this, cells were 'grouped' into neighborhoods with random delays applied. This also allows for more convenient visualization. The higher order

structure of the CA3 network is as yet unknown but, for the convenience of the model, several sets of 'close' cells (cores) were wired together. These cores represent what is likely a realistic convergence phenomenon in a large-scale network (Guzman et al., 2016; Miles et al., 1986). The essential features of the network need to be developed to test this point so for the moment it is left as a necessary simplification. Finally, global inhibition was left intact in the rewired network but the previous local, high speed inhibition was converted to a slow feedback inhibition from the CA3; this is a simplification of the actual situation but the fully accurate rapid feedback would likely require an unrealistic scaling up of the network. (**Fig1-6A)**

Recurrent activity and sustained neuronal activity. 'Cues' were inserted into the simulation via the distal apical dendrites, the terminal zone of the direct projection from the entorhinal cortex, and the mossy fibers. Different frequencies for the two inputs were tested but in all cases a stimulus lasted for 100 msec. The number of firing CA3 pyramidal neurons steadily increased during cue presentation due to recruitment via the associational projections but then stabilized at a maximal value. The latter event reflected an interaction between recurrent feedback and local inhibition. Surprisingly, the population of cells assembled during the presence of the cue continued firing after its cessation (**Fig 1-6C**), in part because the loss of inhibition engaged by the two inputs substitutes for the missing excitation with regard to the maintenance of recurrently active neurons. The maintained spiking of the cells continued for hundreds of milliseconds but then decreased and typically stopped towards one second. Cessation reflected the stochastic properties of the simulation (see above) and so the time at which it occurred varied between simulation runs.

We used high performance cluster computing to evaluate the size of the parameter space in which the above results occur. This proved to be surprisingly large. Inhibitory values, and time delays inserted to mimic the distance between the CA3 cells had incredibly wide ranges often 2-3 fold and 10-20 fold respectively. The LTP vs. excitation ratio was the most sensitive value, with too much excitation leading to the cores rapidly triggering each other.

Interestingly by starting with high excitation values and small LTP values, it was possible to develop a system that would evolve over time as seen below. Size of 'neighborhood' had surprisingly results. As this was raised beyond the tuned values, the size of the stable cluster grew to a ceiling, likely due to the ratio of the inhibitory/excitatory signal, as would be predicted by BCM theory (Bienenstock et al., 1982). But reducing the neighborhood size by even 20% caused a total collapse of the maintained signal, in accord with the idea that the unusual local vs. distant connectivity feature of CA3 promotes sustained signaling. We conclude from this exercise that the observed results are robust and accordingly likely applicable to the actual CA3 network.

Prompted by these results, we conducted the first tests of whether activation of CA3 pyramidal cells during clamp recording in hippocampal slices can result in sustained firing (collaboration with B. Gunn). When a CA3 cell is patched in a slice preparation there are clear miniature activation events (**Fig 1-6D**). It is likely these events are due to the recurrent connections of the CA3. However, it is possible that the reverberation is due to an internal process i.e. the cell activating itself. To test this, glutamatergic transmission was blocked while the cell was patched. As expected the EPSCs were eliminated demonstrating these activation events are caused by external stimulation. (**Fig 1-6E**) Depolarizing current pulses sufficient in size and duration to induce spikes were applied at gamma (50 Hz) frequency for not more than 100 msec. The gamma pattern was commonly followed by an extended period during which the recorded neuron received a series of EPSCs. Repetitive spiking by the recorded neuron was also seen during the period following the initial excitation (**Fig 1-6F**), as expected from the EPSCs.

These findings results establish the plausibility of the results obtained with the simulation and constitute the first direct evidence for the hypothesis that the massive field CA3 feedback system can maintain sustained firing. Notably, slice preparation eliminates much of this system because the pertinent axons exhibit a low level of topography --- the collaterals instead extend

for considerable distances along the septo-temporal axis. This, together with the removal of the large commissural projection from recurrent operations, indicates that the amount of feedback available for sustaining the activity of individual neurons in slices is vastly reduced from that present in vivo. We accordingly conclude that the magnitude and duration of sustained firing described in our modeling work is biologically realistic.

Interactions between two cues. Two cue tests in the model involved activating separate populations of entorhinal projections and two different but overlapping sets of mossy fibers. Each input lasted for 100 msec with varying intervals between them. A first effect obtained was as follows: the sustained activity initiated by cue A continued into the cue B period but then, as the cue B representation built up, most of the originally active cells stopped firing. The observed interaction in part reflects the greater density of interconnections in neighborhoods of neurons than that between widely separated cells (particularly true for commissural connections) and the presence of broadly distributed feedforward inhibition. These arrangements create a type of 'winner-take-all' circumstance in which the most intensely activated clusters (cue B because of now present external input) tend to suppress firing in other clusters (**Fig 1-6G**).

Next, we implemented the above noted LTP rule for synapses between neurons engaged in sustained activity after cue A and those cells brought into play by cue B. As expected, this intensified the cue B response when it occurred within hundreds of milliseconds of cue A in tests after earlier pairing of the two cues. Suppression of activity initiated by the first signal occurred as in (**Fig 1-6G**). Further analyses suggested that such effects could be related to a fundamental form of learning: cued recall. Cues A and B were first associated via the LTP rule and then tested with A cue. Cue A was able to fully retrieve nearly the complete B cue. In essence, the enhanced depolarization produced by the potentiated A:B synapses sufficed to initiate recruitment of a near complete representation of B. (Demonstrated in **Fig 2-1a**)

While maintenance of a cue over time has been demonstrated in cortical models (Compte et al., 2000) ('bump' models), they usually use one cue and test its representation's

robustness in response to noisy inputs. These tend to be models of working memory, and therefore are usually not concerned with the linking of cues over time but with the maintenance of a single cue. We changed this by adding a second cue was to demonstrate that multiple bumps could be stored and retrieved in sequence. Others have developed bump models with multiple inputs; however previous multi-bump models have each bump immediately terminate the bump before it. (Vogels et al., 2005) The current model merges common working memory models with short time retrieval networks, like those seen in Hopfield or Marr networks (Hopfield, 1982; Marr, 1971) and establishes a network that can both hold a stable cue over time and bind it to other cues within itself. Next this model will be expanded to k eep time and to retrieve multiple cues in order.

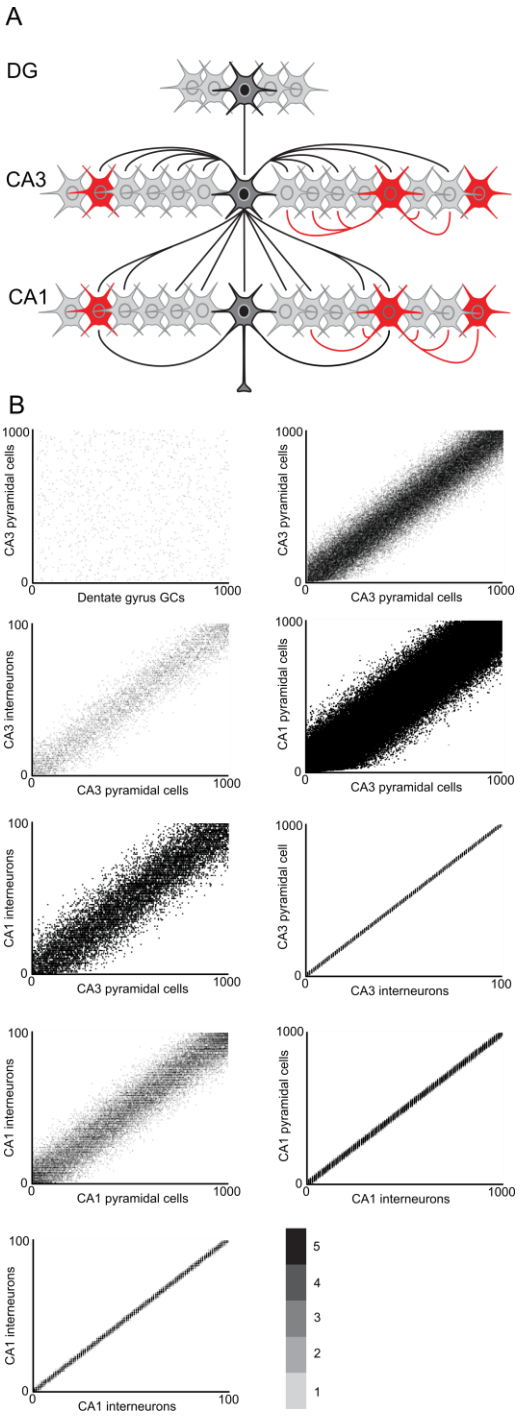


**Figure 1-1 Connectivity of the hippocampal model**

A. Schematic representation of the full DGCA3-CA1 model. Principal cells (grey) and interneurons (red) are illustrated at 1:4 ratio for clarity (instead of the real 1:10). The connectivity is illustrated qualitatively through an exemplar pyramidal cell (dark grey) and interneuron (red) in the CA3 and CA1. B. Connectivity matrixes for all connections within the hippocampal model. Note that the source and target cells are on the x and y axes respectively. The color scale represents the number of multiple connections.

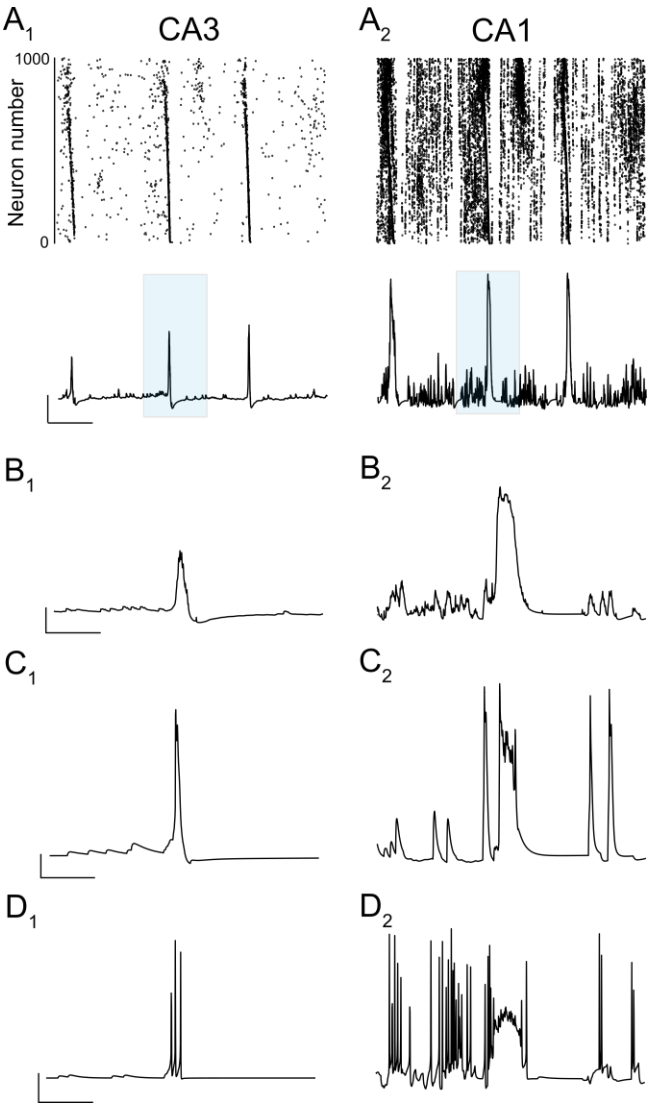


**Figure 1-2 Activation of the hippocampal model generates SPWs.**
A. Neuronal synchronization illustrated by raster plots of spike times for each pyramidal cell in the whole CA3 (A1 top) and whole CA1 (A2 top) array following the activation of the full simulation. The corresponding SPWs generated by 55 neurons in the CA3 (A1 bottom) and CA1 (A2 bottom). A section (shaded area) shows SPWs from the CA3 (B1) and CA1 (B2) on an expanded time scale The pyramidal cell (C1-2) and interneuron (D1-2) spiking pattern from a single neuron during the exemplar SPW for each region (B1-2). Scale bars: (B) y = 10 mV, x = 0.5 s; (C-D) y = 10 mV (E) y = 20 mV, x = 100 ms.

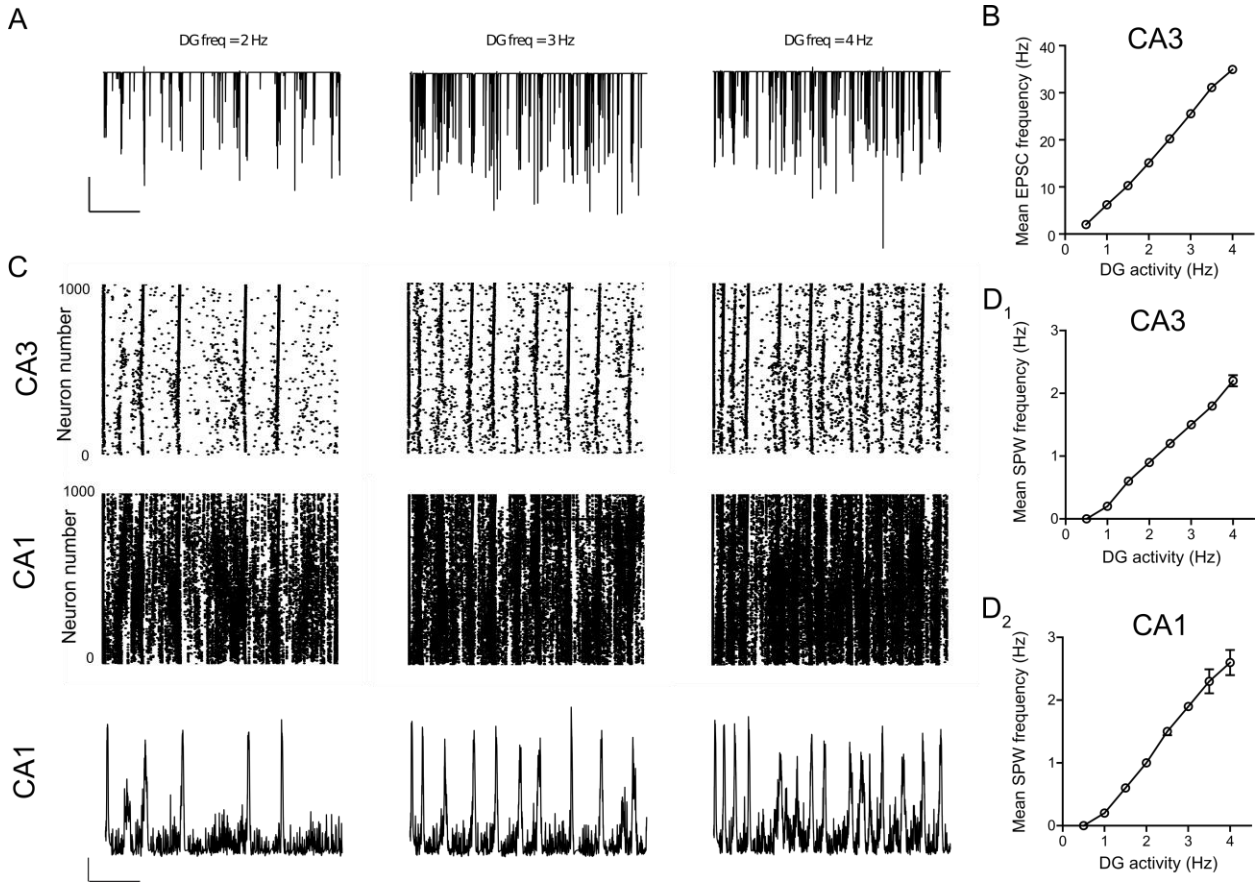


**Figure 1-3 Relationship between mossy fiber activity to the frequency of EPSCs onto CA3 pyramidal cells and the generation of SPWs.**
A**.** Representative sections (5 s) of simulation illustrating the frequency of EPSCs in CA3 pyramidal cells at increasing levels of dentate gyrus (DG) activity. Scale bars y = 20 nA, x = 1 s **B.** Graph illustrating the mean frequency of simulated EPSCs onto CA3 pyramidal cells versus DG activity. **C.** Raster plots of spike times for each CA3 and CA1 pyramidal cell (whole array) in the simulated network at three values of DG activity. Corresponding simulated SPWs generated in the CA1 for each value (bottom). Scale bars y = 10 mV, x = 1 s. Mean frequency of SPWs in CA1 **($D_1$)** and CA3 **($D_2$)** versus level of DG activity.

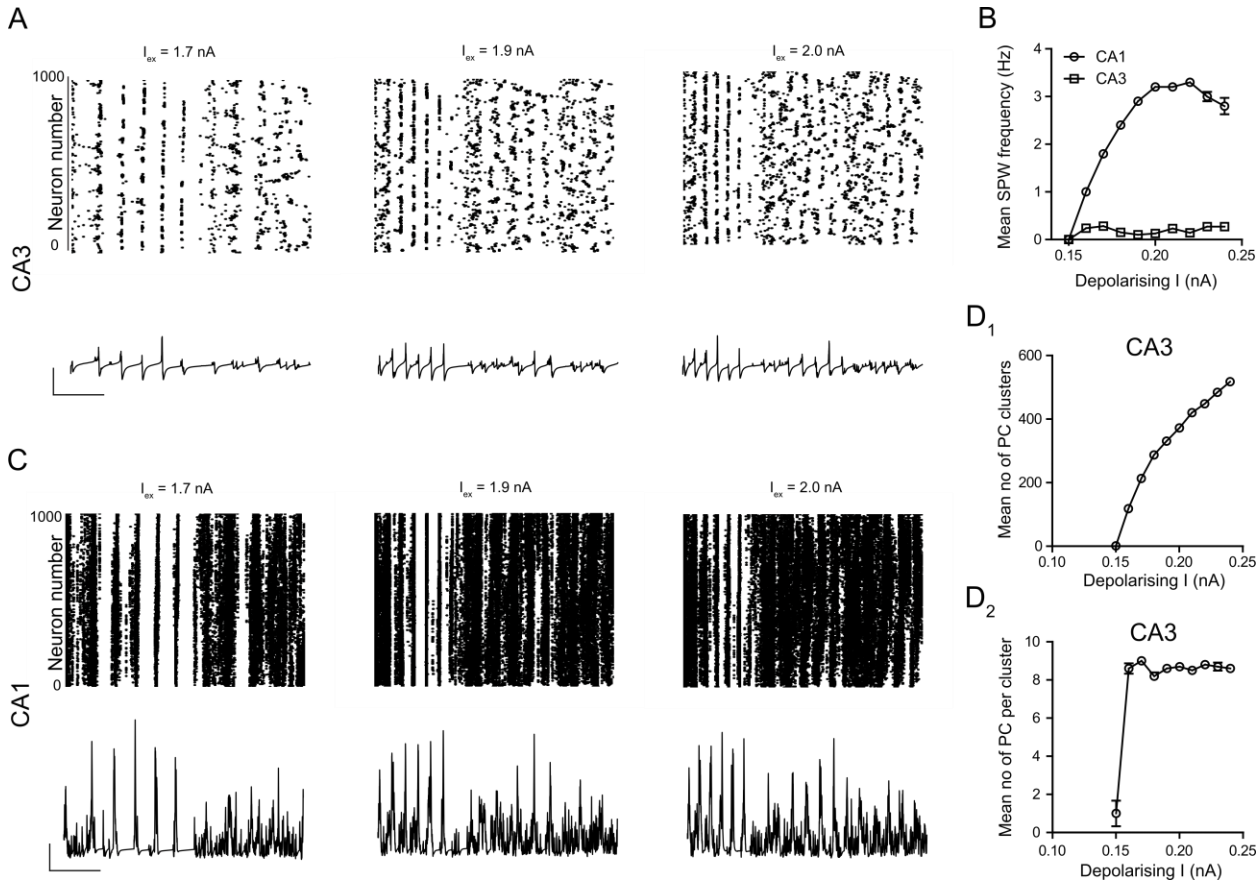


**Figure 1-4 The strength of excitatory synaptic conductance onto CA3 pyramidal cells influences the frequency of EPSCs and the generation of SPWs**
**A.** Representative sections (5 s) of simulation illustrating the frequency of EPSCs in CA3 pyramidal cells at increasing levels of scaled synaptic strength onto these cells. Scale bars y = 20 nA, x = 1 s. **B.** Graph illustrating the mean frequency of simulated EPSCs onto CA3 pyramidal cells versus scaled synaptic strength. **C.** Raster plots of spike times for each CA3 and CA1 pyramidal cell (whole array) in the simulated network at three values of scaled synaptic strength. Corresponding simulated SPWs generated in the CA1 for each value (bottom). Scale bars y = 10 mV, x = 1 s. Mean frequency of SPWs in CA1 **($D_1$)** and CA3 **($D_2$)** versus scaled strength of excitatory synapses onto CA3 pyramidal cells.

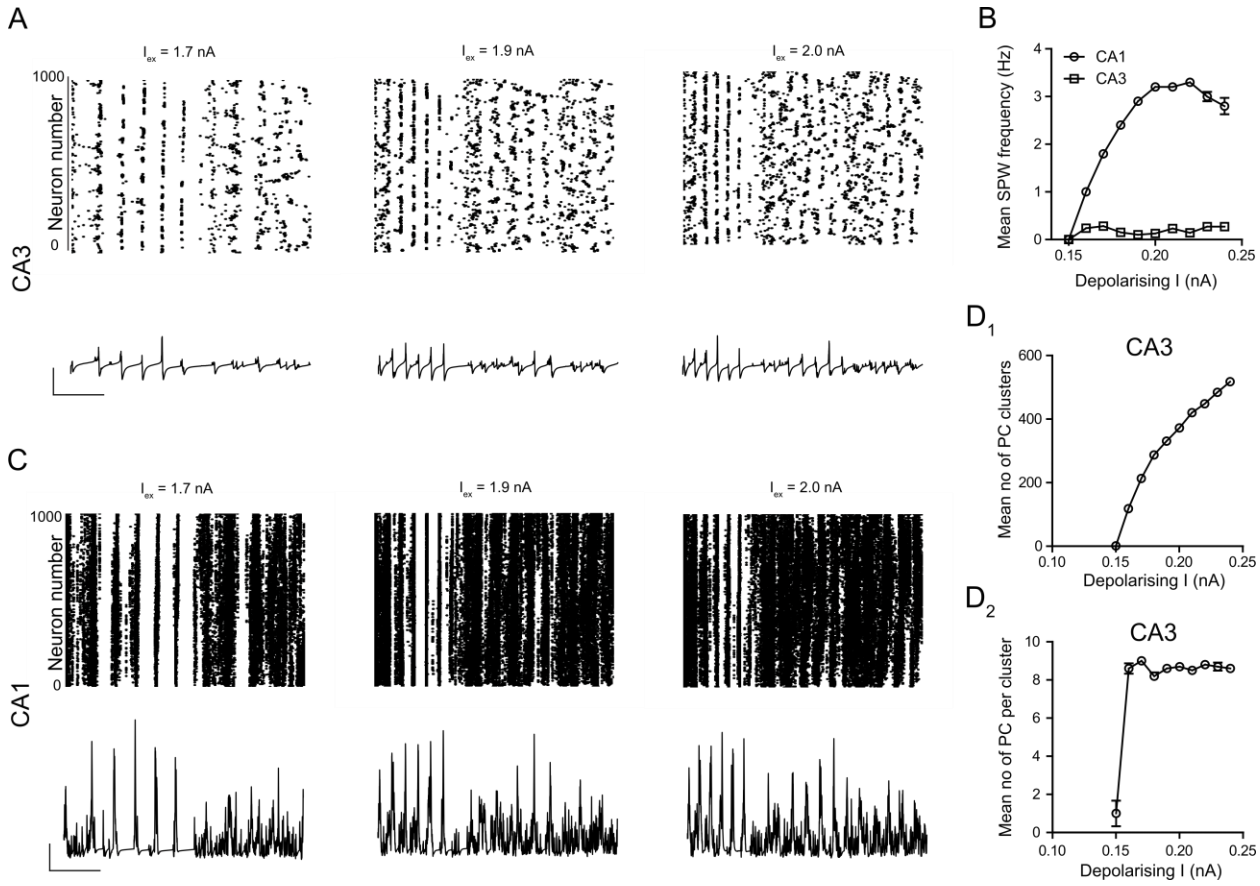


**Figure 1-5 Depolarizing CA3 pyramidal cells desynchronizes CA3 pyramidal cell firing and reduces SPW amplitude.**

**A.** Raster plots (top) of spike times for each CA3 pyramidal cell (whole array) in the simulated network at three values of depolarizing current into CA3 pyramidal cells. Corresponding simulated SPWs (below) generated from 55 cells for each depolarizing current value. Note the decrease in synchronous pyramidal cells spiking in the raster plots accompanied by a reduction in the amplitude of SPWs generated in CA3. Scale bars y = 10 mV, x = 1 s. Graph illustrating the mean number of clusters of spiking CA3 pyramidal cells **($B_1$)** and the mean number of pyramidal cells per cluster **($B_2$)** in response to increasing depolarizing current injection to these neurons. **C.** Raster plots (top) of spike times for each CA1 pyramidal cell (whole array) in the simulated network at three values of depolarizing current into CA3 pyramidal cells. Corresponding simulated SPWs (below) generated from 55 cells for each depolarizing current. Note that in comparison to CA3 the SPW amplitude appears less reduced. Scale bars y = 10 mV, x = 1 s. **(D).** Mean frequency of SPWs in the CA1 and CA3 versus depolarizing current onto CA3 pyramidal cells.

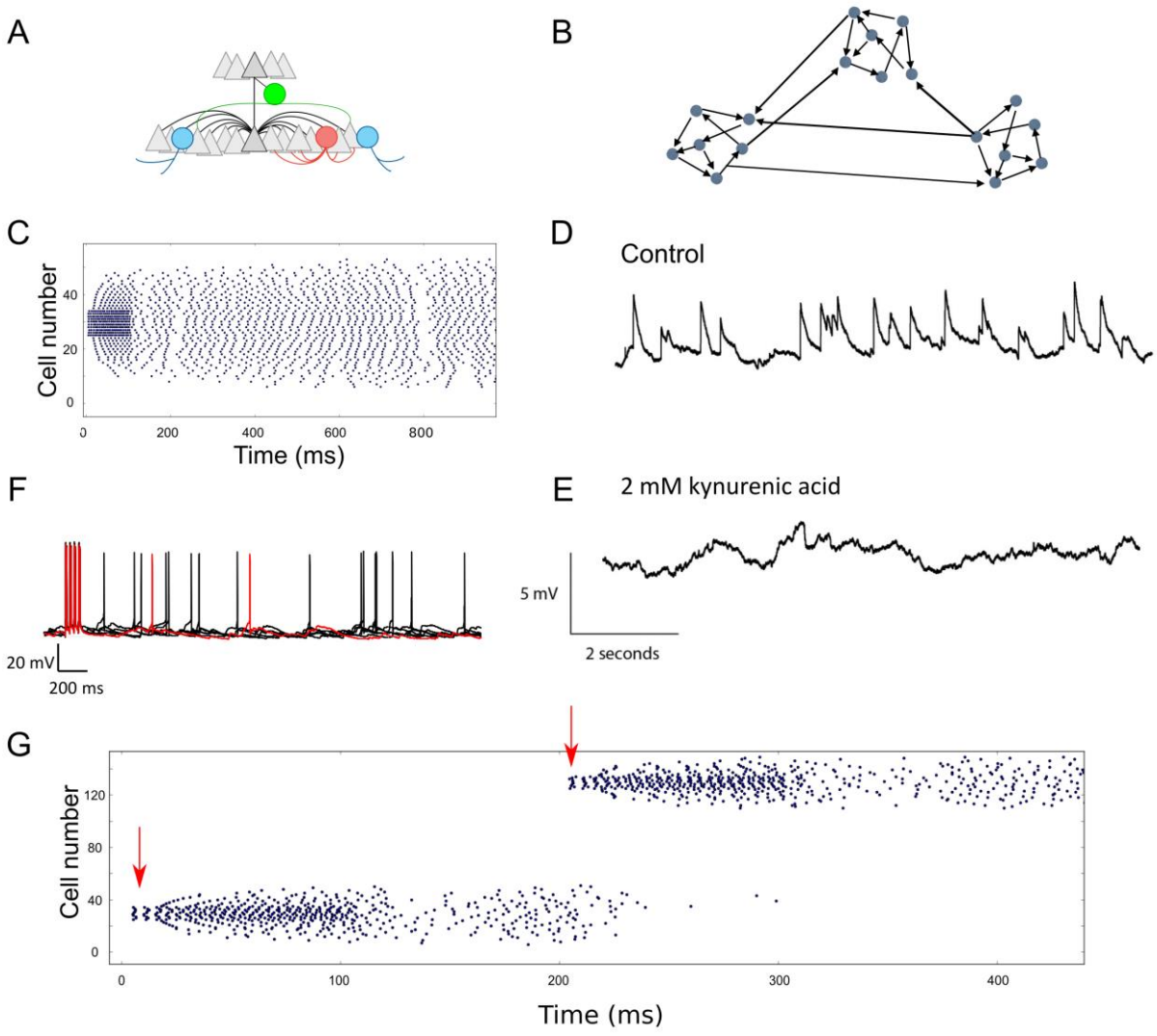


**Figure 1-6 Structure of the CA3 model and electrophysiological tests of predictions from it.**

(A) Schematic of the CA3 model. Triangles represent pyramidal cells that connect heavily to their local neighborhood. The red circle represents local inhibitory cells that feed back to their local neighborhood; these interneurons control both the functional size of neighborhoods and enable shifting between them (see Chapter 4). Blue circles are global inhibitory cells that prevent active pyramidal cells from over exciting other neighborhoods; combined with the influence of local inhibitory neurons, these more widely projecting elements maintain a relatively constant level of network activity. Green cells represent the feedforward inhibition produced by mossy fiber connections with a subgroup of CA3 interneurons. This disynaptic circuit helps to turn off activated cores when new cores are being turned on. (B) Schematic of network architecture. Subgroups of pyramidal neurons strongly interconnect with each other (a neighborhood) and connect more weakly to other, similar functional groupings. This is similar to rich club architecture. (C) Demonstration of network firing; each dot is a single cell. Arrow indicates an initial, transient input that starts the cells cycling; as it terminates, the cells continue firing at their spontaneous network size. This activity continues for an extended period (x axis: msecs) until it stochastically collapses. (D) In vitro whole cell recoding baseline network activity.

Cell is spontaneously activated by recurrent network at baseline. (E) Kynurenic acid blocks this activity. The same cell in the presence of the glutamate receptor antagonist does not receive a lengthy series of EPSPs, indicating that this effect is dependent on locally generated input. (F) A single cell depolarized at the gamma frequency (start of the trace) receives network activity sufficient to cause spiking for up to several seconds; numerous EPSPs that do not produce spikes are evident in the trace. Panels E and F indicate that CA3 neurons do express ‘fire and hold’ behavior. (G) Simulation of two inputs to the model. The second input overlaps the recurrent activity set in motion by the first until feed forward and global inhibition suppress the latter’s. The second then continues firing.

# Chapter 2 Recurrent Networks and Episodic Memory

The previous chapter described the first evidence supporting the hypothesis that anatomical/physiological properties of field CA3 are appropriate for connecting temporally spaced cues. A now considerable literature involving brain imaging studies and work with brain damaged individuals indicates that the hippocampus utilizes linkages across time to integrate sequential information into unitary memory of a type that is far more complex, and cognitively interesting, than that described in Chapter One (Dede et al., 2016). Tulving (Tulving et al., 1988) was the first to formalize the idea that people assemble the complex series of events encountered in real world environments into discrete episodes and to explain how these are distinct from the memory types emphasized in behaviorist theories. Episodes are acquired without prior training and do not involve rewards or external supervision; they incorporate information about the identity of cues (semantic data), spatial relationships between them, and the temporal order in which they occurred ('what, 'where', and 'when') (Clayton et al., 2001; Easton et al., 2012). Sampling tasks involving the 'what' component activate the lateral entorhinal cortex (LEC) that, via its lateral perforant path (LPP), innervates the outer dendritic third of the dentate gyrus' granule cells (van Strien et al., 2009; Wilson et al., 2013). Tests for spatial information ('where') preferentially engage the medial entorhinal cortex (MEC), which projects densely via the medial perforant path (MPP) to middle third of the same dendritic field (Hargreaves et al., 2005). Lesion and recording studies involving rodents confirm that 'what' and 'where' data are transferred to hippocampus by the two subdivisions of the entorhinal cortex (Hafting et al., 2005). These observations fit well with well-established connections of the entorhinal cortex. The region has dense two-way relationships with association cortices; these include, but are not restricted to, complex spatial representations relayed to the MEC and semantic ones transferred to the LEC. The LEC is also closely related to the piriform cortex, a simple form of associational cortex that processes olfactory cues (Chapuis et al., 2013).

The critical question of how the temporal component of an episode is added returns us to the discussion of cue associations included in Chapter One. Imaging studies report that temporal ordering activates fields CA3 and CA1 (Eichenbaum, 2014; Salz et al., 2016). Given that the former is by far the major source of input to the latter, it is reasonable to assume that processing of time engages CA3 and its massive recurrent system with the output being fed into CA1. However, it has been argued that CA1 performs the essential computations through direct interactions between it and the entorhinal cortex (see above).(Jochems et al., 2013). This hypothesis, in its simplest form, requires the unlikely corollary that the observed CA3 activation is irrelevant to processing of cues by CA1. The work described below investigated whether recurrent activity of CA3 and its transmission to CA1 suffice to produce complex episodic phenomena.

A critical feature of episodic memory involves retrieval of sequential information, such that activation of a representation that occurred early in a series leads to the appearance of the encodings associated with later, related events. An individual questioned about whether they had encountered a specific item will typically replay a fraction of an episode so as to find the pertinent data, an everyday operation that illustrates the immense capacity of this form of storage.(Dede et al., 2016) Our studies began with this essential retrieval feature of episodes.

## 2-1. Retrieval of cue identity and temporal information contained within an episode.

Cue information, temporal order, and intervals. We used the LTP rules described in Chapter One to encode a sequence of three cues separated by 300 msec and then tested the network when only of the first of these was subsequently presented. Presented with only the first cue, the revised model first generated the expected cue A response, which persisted for about 100 msec before a second representation corresponding to cue B emerged. This led to a cessation of the population associated with the first stimulus. These events were followed by the delayed appearance of the cue C population of neurons (**Fig 2-1a**). These first experiments

establish that an approximation of the CA3 associational system can perform retrieval and so provide a fundamental operation of episodic memory.

Next we tested if the model incorporates information about the relative delays between the cues that occurred during encoding. Cue B followed Cue A by 150 msec while cue C was delayed by 500 msec during sequence acquisition. During retrieval, B emerged after a shorter delay than that for C (**Fig 2-1b,c**); thus the system captured information about relative time in the learned sequence. Analysis indicated that this unexpected effect reflected the following. During acquisition, the population of neurons activated by the now present cue recruits neighboring cells, a process that continues after the input terminates. While the size of the maintained collection is reasonably constant, individual cells that are active at any given time segment varies. This means that LTP occurred between those (different) cells activated by the B input and the particular A neurons that were firing at that particular time. During retrieval, the cue A population cycles though its members until a sufficient number of those connected (via LTP) to the B group are engaged at about the same time to drive B neurons into the active state (**Fig 2-1d,e**). Longer delays between cues during learning results in ever greater divergence between the population responding to cue A and the cells active when cue B arrives. Thus, longer cycling time during retrieval is needed before the A-B neurons are engaged.

The temporal component of an episode includes both the order of the elements in a sequence but as well as information about expected delays. The above results lead to the remarkable conclusion that both of these seemingly complex operations can be executed by a simplified version of the basic design of field CA3.

Time compression. A salient feature of episodic memory is that replay can take much less time than the actual experience that led to its formation (Eichenbaum, 2014; Nádasdy et al., 1999). This feature occurred in some runs of the basic CA3-CA1 simulation (**Fig 2-1f**). Acquisition occurs when an attentive agent is sampling a real world circumstance and processing in the hippocampus necessarily dominated by the pace of events. Retrieval on the

other hand involves an effort to activate stored content, typically in the absence of engagement with surroundings. Switching between these hippocampal states likely depends on cholinergic input from the septum, which is distributed largely to the dentate gyrus and field CA3. Released acetylcholine causes a modest and slow increase in the excitability of pyramidal cells that appears to be mediated by muscarinic receptors. We are currently testing predictions from this aspect of the modeling work using optogenetic stimulation of the septal cholinergic projections to field CA3.

Hypothesized role of field CA1. The above results establish that the basic features of field CA3 are capable of encoding and retrieving essential elements of episodic time including cue order, relative intervals between cues, and temporal compression. The question then arises as to what types of further processing occur in field CA1 when these events are transferred to it via the massive projections from CA3. One intriguing possibility is that the region uses LTP to encode representations of cue-time-cue triads that are then used to recognize such episodic items on future occasions. The sequential signals arriving from CA3 during the first encounter with the serial events will strengthen their connections with CA1 preferentially on those neurons also receiving direct input from the entorhinal cells activated by the individual cues. Prior modeling work showed the potent basket cell mediated feedback inhibition creates a 'winner-take-all' situation in which initially activated neurons block firing by their neighbors (Ambros-Ingerson et al., 1990; Coultrip et al., 1992). This device acts to ensure that a fixed and small population of cells is active at any given moment in time. The net result of these arrangements is that a particular spatio-temporal pattern developed in CA3 will be associated with a unique sequence of cues. Note that a subsequent presentation of any item in the sequence is likely to activate a major portion of this CA1 representation for the entire episode.

This argument is consistent with the well-described anatomical/physiological characteristics of field CA1 and the CA3 features discovered in the modeling work described above. We intend to test it using biophysical simulations. But as it stands, the proposed

hypothesis provides the beginnings of an explanation for a very difficult question relating to episodic memory: how does the cortex carry out computations involving large numbers of episodes, each of which contains an enormous amount of information? The hypothesis advanced here is that field CA1 provides the cortex with a unitary signal for a given episode along with compacted data relating to its content. The first of these elements could then be used for rapid computations (e.g., placing the episode in a category) while the details are retrieved via slower processes of the type described above. We will return to these ideas in a later section (Chapter Four) concerned with where in hippocampus most of LTP-like synaptic modifications occur during episodic learning.

Experimental tests of the role of CA3 in the acquisition of temporal information. We conclude from the above that field CA3 performs the essential operations required for incorporating a temporal element to an episode. There is very little experimental evidence that bears directly on this point. Chronic recording studies have described CA3 and CA1 cells that fire in a time related manner in rodent tests involving serial odors but these studies used extensive reward based training (MacDonald et al., 2011; Salz et al., 2016). Other studies have used highly supervised or extremely simple behaviors such as context fear conditioning or trace blink conditioning to test time processing (McEchron et al., 2003; Modi et al., 2014). But given that episodes are encoded in humans in a routine and unsupervised manner, it is questionable whether the findings from the recording studies are applicable to the questions raised by the modeling work. Accordingly, experiments were conducted using transient, unilateral silencing of field CA3 and serial cue protocols that do not require prior training or explicit rewards (collaboration with B. Cox). As described, CA3 receives about 50% of its recurrent feedback from commissural projections. It is evident from our simulations that removal of this input will drastically reduce circulating activity in the otherwise intact contralateral CA3 while leaving feedforward operations (entorhinal cortex>dentate gyrus>CA3>CA1) operations intact.

The behavioral procedures developed for the experiment are illustrated in **Fig. 2-2b,d**. The animal was given free access to two identical odorants for 3 minutes, removed from the chamber, and then returned two minutes later to explore a second pair of odors. This was repeated for a third and fourth odor, resulting in an A:A, B:B, C:C, D:D sequence. A test trial in which A was paired with D (A:D) was then conducted five minutes later. The animals exhibited a clear preference for D in the test phase, indicating that they had remembered A despite the intervening cues and so had acquired a simple form of order information. We then injected Gi-DREADD virus into the CA3 of one hippocampus followed by a three-week period to allow for expression (**Fig 2-2a**). Electrophysiological assays confirmed that infusions of the DREADD agonist clozapine-N-oxide into slices from transfected animals caused a pronounced (>50%) reduction in fEPSPs. Peripheral administration of the agonist, but not vehicle, prior to odor sampling entirely eliminated the selection of cue D relative to cue A in transfected (**Fig 2-2c**).

In contrast, unilateral transfection had no detectable effect on the acquisition of 'what' data. For these experiments, animals were given an A:A, B;B, C:C sequence and then tested for discrimination between familiar odor A and a novel odor D (A:D). Time spent exploring the novel odor were comparable for the two groups (**Fig 2-2d,e**). That the unilateral hippocampus suffices for the 'what' problem is as expected given that bilateral silencing the LEC is required to block acquisition in this paradigm. In all, the results accord with the prediction that recurrent networks in field CA3 play a central role in processing of temporal order.

The above data demonstrates the CA3 is capable of maintaining and changing cues over time. This change gives the CA3 the ability keep track of time, as a signal's evolution corresponds to the time since the cue was activated. The evolution of a signal from an initially stable bump is often seen in 'bump' models when any unevenness is introduced in a model with no LTP-like mechanism. This evolution is typically seen as a flaw in these models or is used as a mechanism of oscillatory activity. (Vogels et al., 2005) However, as demonstrated above, this

is a potential mechanism of time keeping. The rate the signal propagates is relatively constant due to excitatory/inhibitory balance.

Physiologically the CA3 was shown to perform long reverberations on repeated stimulation. The exact meaning of these reverberations and the network architecture that allows the CA3 to be activated seconds later is unclear. These features and how they are represented or can be incorporated in to the model will need to be further explored in mathematical analyses of real-scaled, computationally intractable large networks. However, these physiological results demonstrate that even an extremely reduced CA3 slice preparation has large scale network convergence and continued activation. This implies higher order structure to the CA3 which has recently become a major topic of research (Guzman et al., 2016).

Finally, the above behavioral data demonstrates that not only is the CA3 required for episodic-like memory but also that the complete CA3 is required. Eliminating half the inputs of the CA3, and most importantly the commissural system, specifically eliminated animal's ability to learn 'when' memory. While no commissural system was included in the model, elimination of a small number of inputs in the model caused it to collapse.

These three lines of evidence will need to be reconciled using network analysis and in vivo recording. What is clear is that the CA3 contains machinery that could support time processing, can reverberate electrically on extremely long time scales, and requires its full architecture to process 'when' memory. To further explore this processing and storage we examined where memory was stored at the synaptic level across the hippocampus.

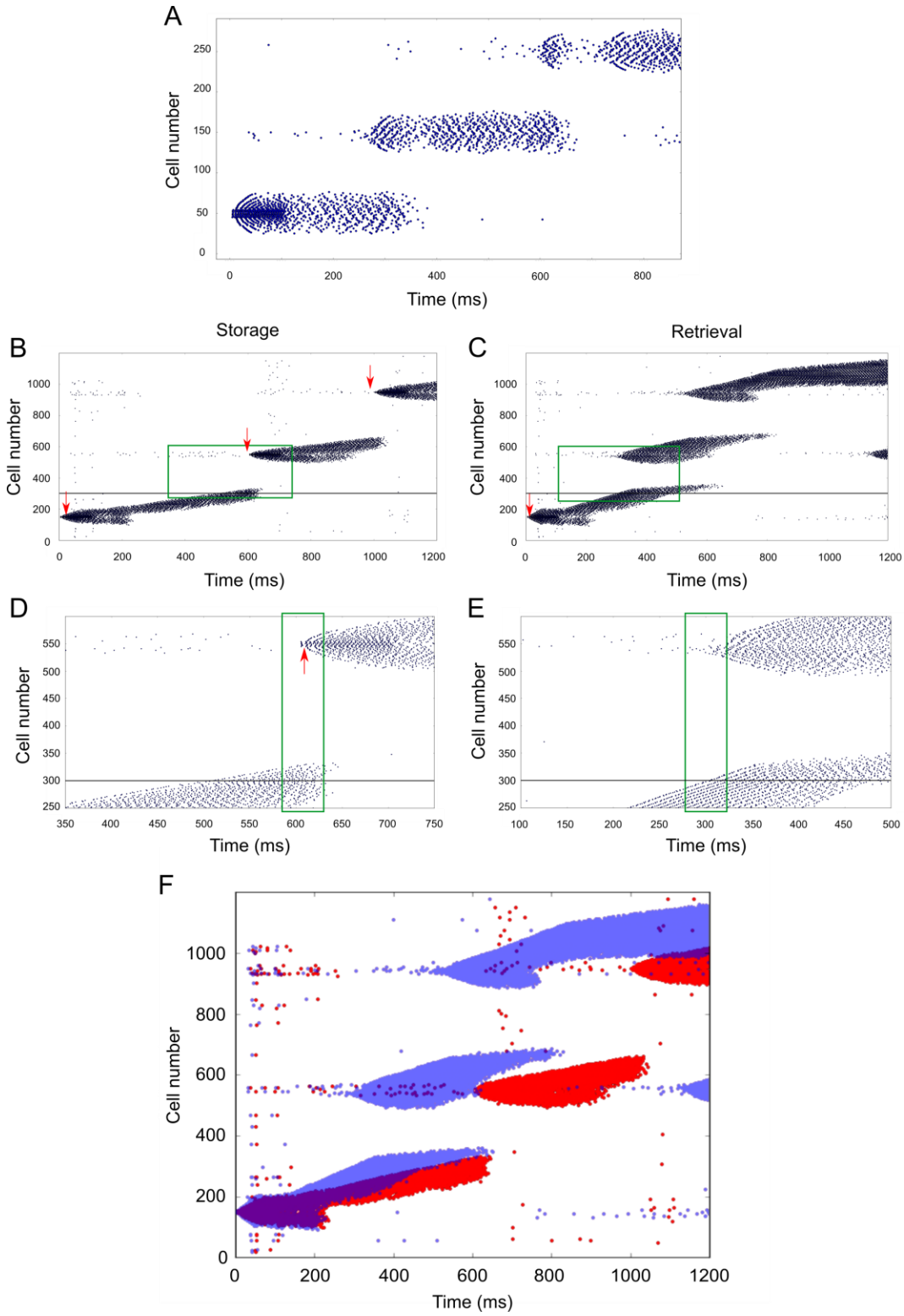


**Figure 2-1 Retrieval of a learned sequence by a CA3 model: order of cues, relative intervals between them and time compression**

(**A**) The model was trained on a sequence of three cues during which LTP rules were active. Subsequent presentation of the first cue alone led to sustained activity that eventually activated

the cells associated with the second cue; note that this was associated with inhibition of the activity initiated by the first. After a delay, activity associated with the retrieved second cue triggered cells representing the third cue, with suppression of cue B. (**B**) Evolution of signals over time with slightly modified LTP rules during learning. The potent feedforward inhibition from the mossy fibers stimulated by a brief cue (red arrow) was allowed to reduce the strength of LTP between CA3 neurons activated by the same fibers. Additionally, the magnitude of potentiation was lowered for all CA3:CA3 contacts during learning. Note that these changes resulted in a response to cue A that evolved over time by spreading to neurons other than those initially activated cue A. As above, presentation of cue B terminated the activity triggered by A and produced a signal that evolved over its own time course. These events repeated when cue C was delivered during learning. (**C**) Retrieval of the signal in panel 8B following reactivation of cue A only (red arrow). The signals were reactivated in the correct order and maintained their relative temporal spacing. (**D,E**) Zooms of panels 8B and 8C to show cells active during learning and retrieval; the horizontal line marks the position of cell #300. The green box includes the population of cells around neuron #300 (horizontal) that were active during encoding. When a sufficient number of the same cells are reactivated during retrieval, they cue the neurons in the storage core for cue B. (**F**) Retrieval is time compressed relative to storage. Panels 8B (red) and 8C (blue) overlaid. The cues from panel 8C occur faster than their original storage rate, both by moving through their time evolution at a higher rate and by reactivating the next cue in the sequence earlier in the time range.

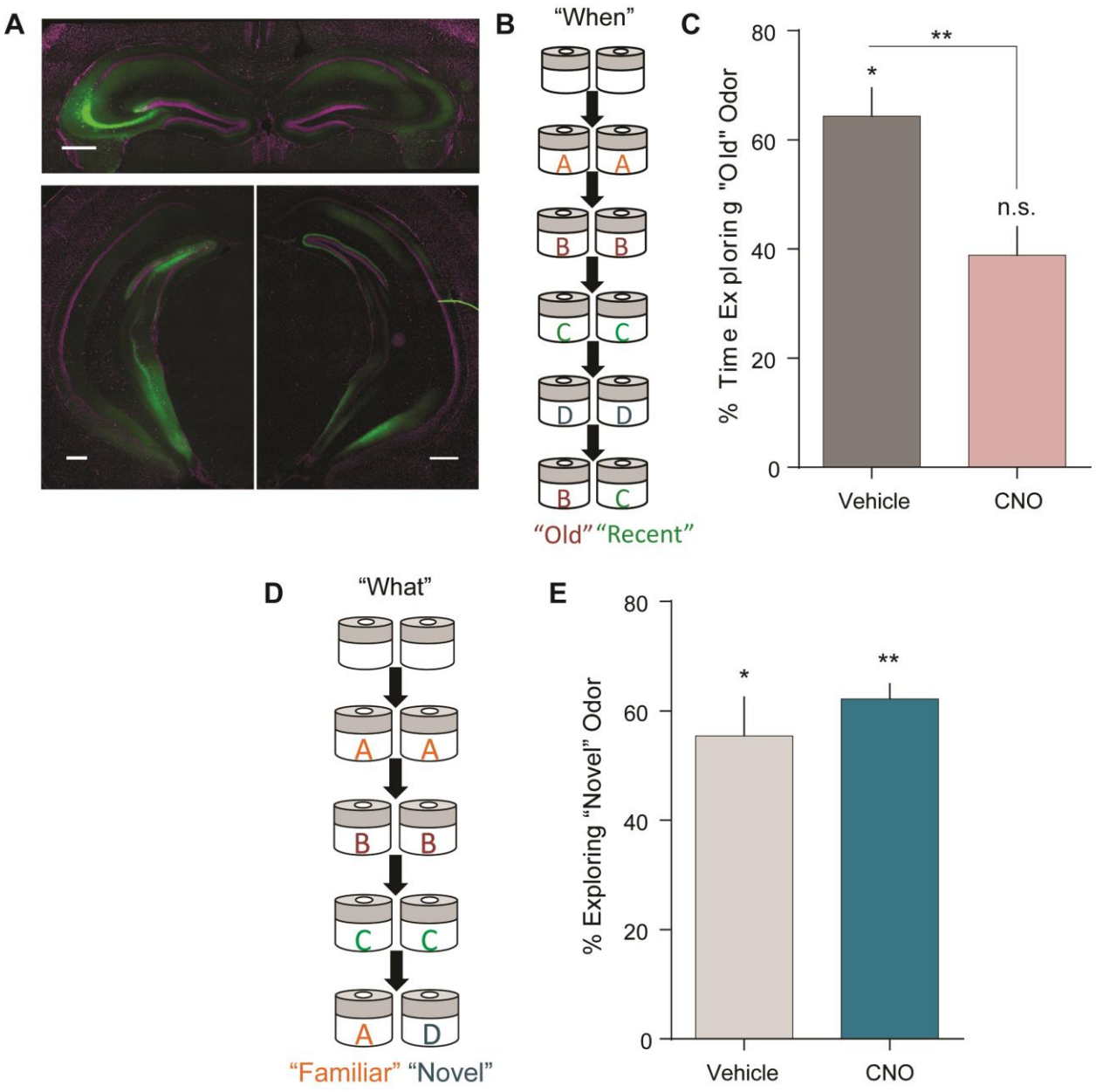


**Figure 2-2 "When" learning but not "What" learning is dependent on unilateral CA3**
(A) An AAV-Gi-DREADD was injected into dorsal (top) and ventral (bottom) CA3 unilaterally which resulted in receptor expression of CA3 cells and their ipsilateral and contralateral projections (green). Scale bars = 500 mm. (B) Illustration of the serial odor "When" Task. (C) Animals injected with Gi-DREADD in the unilateral CA3 were tested in the "When" Task paradigm after Vehicle or CNO treatment. Vehicle animals spent 64±6% of their total exploration time sampling the "old" odor more than the "recent" odor (*p<0.05, n=5, paired t-test), while the CNO treated animals did not show a bias for the odors (n.s. : not significant., n=6, paired t-test). The difference between the two groups was significant (**p<0.01, unpaired t-test). (D) Illustration of the serial odor "What" Task. (E) CA3 Gi-DREADD injected animals were tested in the "What" paradigm. Vehicle animals spent 63±5% more time with the "novel" odor (*p<0.05, n=7) and CNO animals spent 62±3% (**p<0.01, n=7). There was no significant difference between the two groups.

# Chapter 3 Routine Episodic Learning in Complex Environments

Episodic memories in real world circumstances are encoded without past training or explicit rewards (unsupervised or experiential learning). They differ in this important regard from the cue-response-reward type of learning used in the great majority of studies using laboratory animals and also commonly studied in humans. Accordingly, the behavioral studies described in Chapter 2 used unsupervised experience to separately analyze the acquisition of three basic elements ('what', 'where', 'when') of an episode. However, these elements occur together in natural environments along with other features. We thought it necessary to develop behavioral tests that capture these features in order to advance the analysis of how the hippocampus contributes to the formation of episodes. These studies brought us into contact with another large question that is vital to episodic learning but poorly studied in animals: transfer of learning from past experience with complexity.

We attempted to develop a testing apparatus in which rats deal with a very complex situation by dividing their behavior into discrete episode-like forays and then measuring their unsupervised learning. Success in this has opened the way to studies on the role of the hippocampal pathways discussed above in processing sequential sematic, spatial, and temporal information in conditions approximating those encountered in nature and in which humans routinely organize the flow of experience into episodes. A next step for such studies is to ask whether synaptic encoding of information is localized to particular intra-hippocampal connections or instead is uniformly distributed. This question will be addressed later in this thesis.

## 3-1. Episode-like learning in a complex environment.

Testing apparatus. Our attempts to develop a testing situation in which rats divide their behavior into numerous episodes began with a straightforward extension of a well-known phenomenon: the reduction of spontaneous locomotor activity over time by rats in a novel open

field. While open field testing was originally introduced (Hall et al., 1932) to measure emotionality in rodents, it became widely used as a simple test for memory involving the speed at which well-handled rodents become familiar with a new environment (Walsh et al., 1976). Traditionally termed “habituation”, this behavior serves as a simple example of unsupervised experiential learning in animals. We extended this simple paradigm to a complex novel environment including internal barriers, passageways, local objects, and distant visual cues. Prior work (Eilam et al., 1989) demonstrated that rats in open fields spontaneously choose a “home base” location from which they make exploratory forays and to which they tend to return at a higher rate of speed; based on this result and to ameliorate the aversive component of open-field testing we included a small, dark, enclosed “refuge” chamber to serve as an ethnologically relevant home base candidate attached to the complex environment **(Fig 3-1E,F**). Exploration in the complex arena was thus voluntary, and divided by the animals themselves into discrete forays (**Fig 3-1G**).

Our initial experiments produced surprising results: rats given extensive handling twice daily for a week showed very little evidence of learning during two 30 minute sessions separated by one day. Their exploration rates changed only slightly on day one (short-term memory: habituation) and behavior on day two was little changed from day one. It thus appeared that the apparatus was too complex to be acquired in 30-minute periods. We accordingly ran a full scale study using three large groups: 1) six daily five-hour exposures to an enriched environment (EE group); 2) an equivalent period of free access to exercise, in the form of running wheels (WR group); 3) twice daily episodes of standard handling (SH group) (**Fig 3-1A,B,C,D**). The analysis below begins with the classic measures of open field learning in terms of habituation rates (reduction in rates of exploration as measured by distance traveled and changes in this measure over time), and then turns to analysis of the forays.

Short-term memory. Exploration within the simple refuge compartment as measured by distance travelled began at a high level then progressively and sharply decreased during the

first 15 minutes of the session and changed little afterwards for all groups **(Fig 3-2A**), exhibiting the classic habituation curve of a rat in an unstructured open field. It thus appears that past experience has relatively little effect on rapid habituation within a simple environment.

In the complex arena, Standard Housed (SH) rats conducted considerably *more* exploration as measured by total distance travelled over the entire 30 minutes (110.0 ± 4.6 meters) than did either Enriched Environment (EE) (77.4 ± 4.1 meters) or Wheel running (WR) (75.4 ± 3.9 meters) rats ($p<0.0001$, **Fig 3-2B**). Yet SH animals exhibited no significant decrease in exploration of the arena over the course of the session (unlike their behavior within the refuge compartment), showing a flat, non-significant habituation curve ($r^2 = -0.11$, $p = 0.5$) over the 30 minute test; the WR group showed a moderate degree of habituation ($r^2 = 0.8$, $p < 0.01$), while that for the EE group ($r^2 = 0.97$, $p = 0.0001$) was steeper and much more pronounced (**Fig 3-2C**). These group differences (**Fig 3-2D**) were highly significant ($p<0.0001$), with the slope of the EE group's curve greater than that of SH or WR animals ($p<0.001$ for both comparisons, Tukey post hoc tests). We conclude from these results that past experience with complexity enables rapid learning of a new, high choice environment.

Long-term memory. Despite extensive exploration of the arena on day one, total distance traveled by SH animals was only slightly reduced (<10%) in a second session conducted 24 hours later; in contrast, EE rats' travel through the arena decreased by approximately 30% across the two days (**Fig 3-2E**). Prior exercise did not reproduce the effects of enrichment on total exploration: there was no significant change from day one to day two for these animals. Similarly, the habituation curve for SH rats after the first 5 minutes was only slightly steeper on day two relative to day one (**Fig 3-2F**) and did not approach that for the EE group on day one or two. In all, evidence for long term memory in the standard handled rats was modest. In marked contrast, the EE group exhibited a robust between-days change in habituation: exploration decreased dramatically between the first and second 5 minute time

intervals on day two ($p = 0.0003$), an effect not seen on day one **(Fig 3-2G**). Habituation on day two by the WR animals was not detectably different from that on day one (**Fig 3-2H**).

Numerous studies have shown that exploration of an unstructured open field by rodents produces clear evidence of long term memory (reduced activity) in tests carried out on subsequent days; the weakness or lack of such effects for the SH and WR groups in our study indicates that stable encoding is much more difficult for animals confronting a complex arena. It appears that prior learning by the EE cases, though acquired in a very different complex environment, proved to be transferable to the novel circumstances such that encoding on day one was both rapid and enduring.

Notably, the EE and SH rats were not detectably different on multiple, conventional measures of arousal and anxiety including movement speed, percent time active, preference for darkened spaces, and defecation (**Fig 3-3**). These findings indicate that differences in arousal and anxiety were not likely to have contributed to the learning differences between EE rats and the other groups.

**3-2. Transfer from past experience shapes search strategies.**

The rapid learning by the EE group raised the possibility that their past interactions with a very complex environment resulted in search strategies that were sufficiently flexible to be applicable in new challenging circumstances. We investigated this by closely examining the patterning of exploration by the EE and SH rats. As noted, the inclusion of the small, dark, enclosed, and empty chamber (‘refuge’) to serve as an ethologically relevant home base attached to the complex environment led all three groups of to divide their behavior into distinct exploratory episodes, here called ‘forays’, into the complex arena, punctuated by stays of varying duration within the (simple) refuge.

The total number of exploratory forays made during the first session by SH animals was not significantly higher than the EE group ($p>0.07$) but was greater than in the WR animals (**Fig**

**3-4A**). Like distance traveled, clear group differences emerged in how foray counts evolved over time during the session. This was assessed by dividing the session into 10 minute time intervals and assigning each foray to the interval in which it began. In the SH group foray counts changed little over the three intervals (slope: -0.10 ± 0.03), but EE rats began with a high foray count, dropped by half during the second time interval, and halved again in the final ten minutes (slope:-0.41 ± 0.03) (**Fig 3-4B**). WR rats were similar to SH for the first two intervals but showed a decrease in foray initiations in the third, resulting in a slightly steeper habituation curve overall (-0.19 ± 0.03). The difference in slopes between the EE and other groups was highly significant. These results suggest that rats with past experience in dealing with complexity implement a different exploratory strategy for investigating a new and challenging environment than rats without such experience.

Foray counts across days were nearly constant for SH (20.2 ± 0.9 to 20.0 ± 0.8) and WR (14.9 ± 0.7 to 15.2 ± 0.9) groups, a further indication that these animals did not form robust long term memory on day one, while EE rats showed a marked decrease in the total number of forays between the two test sessions (17.5 ± 0.9 to 12.3 ± 1.2) (**Fig 3-4C**). Most of the between-days decrease in forays seen in the EE group (~60%) occurred during the first 10 minutes of session two (**Fig 3-4D**); the other two groups did not reduce their forays during this period (**Fig 3-4E**). It thus appears that EE, but not SH or WR, animals learned enough about the complex test environment on day one such that they quickly recognized it and so were less inclined to initiate exploratory forays 24 hours later. Long-term memory effects in the latter two groups were minimal.

Next, we examined foray characteristics during the first session in an attempt to identify features that could account for the enhanced learning by the EE group. The space was divided into a 7x7 grid (49 cells) and the percentage of these entered by the animal measured for each of its forays. All rats made forays using a range of different arena coverage values, with foray counts peaking for forays between 40-60% coverage for rats in all groups (**Fig 3-5A**). However,

EE rats shifted their distribution away from high-coverage (> 60% coverage) forays (**Fig 3-5B**) compared to the other two groups, while making approximately the same number of low and moderate coverage forays as SH rats (counts of forays with coverage < 60%, p=0.9, t-test; see **Fig 3-5A**); by contrast WR rats made fewer forays overall (as we saw above, **Fig 3-4A**) but their distribution of forays of different coverage values was similar to that of SH animals, shifting the entire curve downwards (**Fig 3-5A**).

We next considered the pattern of forays used by the animals to first attain full coverage of the arena during initial exploration. Accordingly, the subset of initial forays cumulatively covering ≥ 90% of the arena was examined for each animal; one rat in each group had values that were more than 10 SDs from the mean of the remaining 30 and so were excluded from the analysis. Full coverage occurred relatively quickly. EE rats required 5.5 ± 0.3 forays with the last of starting at 3.5 ± 0.4 minutes; SH animals used a similar number of forays (5.2 ± 0.3) but with the last of these at 5.0 ± 0.4 min (p=0.011 vs. EE). The WR group were extremely variable on these measures: 41% of the animals (11/27) covered the arena quickly (1.35 ± 0.16 min) with a small number of forays (2.2 ± 0.2) while the remainder had much higher values (5.6 ± 0.5 forays, 8.7 ± 1.2 min).

As expected from the above, the mean duration of the forays used for initial coverage of the arena was markedly lower in the EE group: 31.0 ± 1.8 seconds (s), versus SH rats 49.0 ± 3.8 s and WR 73.7± 12.6 s (p < 0.0001, **Fig 3-5C**). The EE group rats thus adopted a strategy of shorter, more frequent forays which, when combined, cover the same cumulative percent of the arena, compared to the other groups.

Do the forays made by EE rats also tend to overlap less? That is, do the above results suggest that EE rats divided the arena into smaller, more distinct exploratory portions per foray? To investigate this, we measured the extent to which successive forays overlapped, expressed as the percent of grid cells visited in the current foray that were not visited in the immediately previous one. For the initial set of forays first leading to full coverage of the arena described

above, EE rats' foray distinctness was, on average, slightly but significantly higher (EE: 63.2 ± 2.2%; SH: 58.9 ± 2.3%; WR:54.4 ± 2.9%; p=0.009, ANOVA, with EE vs SH p=0.04 and EE vs WR p=0.01, WR vs SH (p=0.8), Tukey post-hoc tests). Indeed this result held for the entire session (p=0.003, **Fig 3-5D**). Of interest, this measure showed a weakly negative correlation with foray number (that is, overlap tended to increase slightly for later than earlier forays) that was stronger for EE rats than the other two groups (p=0.02, **Fig 3-5E**).

Finally, we tested for group differences in movement choices within individual forays using a line-crossings measure. A 10x10 grid superimposed over the video image of the arena allowed measurements of the number of times each rat repeated crossings of the same grid segment during individual forays. The EE rats showed a substantially larger proportion of forays in which most (≥75%) line crossings were unique than did the WR or SH rats; WR and SH groups were not different on this measure (p<0.003, **Fig 3-5F**). It thus appears that a primary effect of prior environmental enrichment, but not exercise, is to increase the likelihood of forays in which rats do not repeat material sampled in the immediate past.

The above findings indicate that the rapid learning by the EE group during the first session was not due to more exploration of the test arena - to the contrary. Instead, relative to the SH and WR rats, these animals began with a higher frequency of briefer, less repetitive forays to explore the arena. This suggests that the material transferred from earlier complexity included a flexible strategy for dealing with high dimensional circumstances.

In all, rapid learning using discrete sampling episodes requires the individual to have a history of interacting with complicated environments and well-developed internal rules for investigating unfamiliar situations. The enormous power of episodic memory does not occur in isolation but rather occurs in the presence of guidelines acquired over a lifetime. That rats exhibit simple versions of these phenomena is surprising but encouraging with regard to experimental work on fundamental components of cognition.

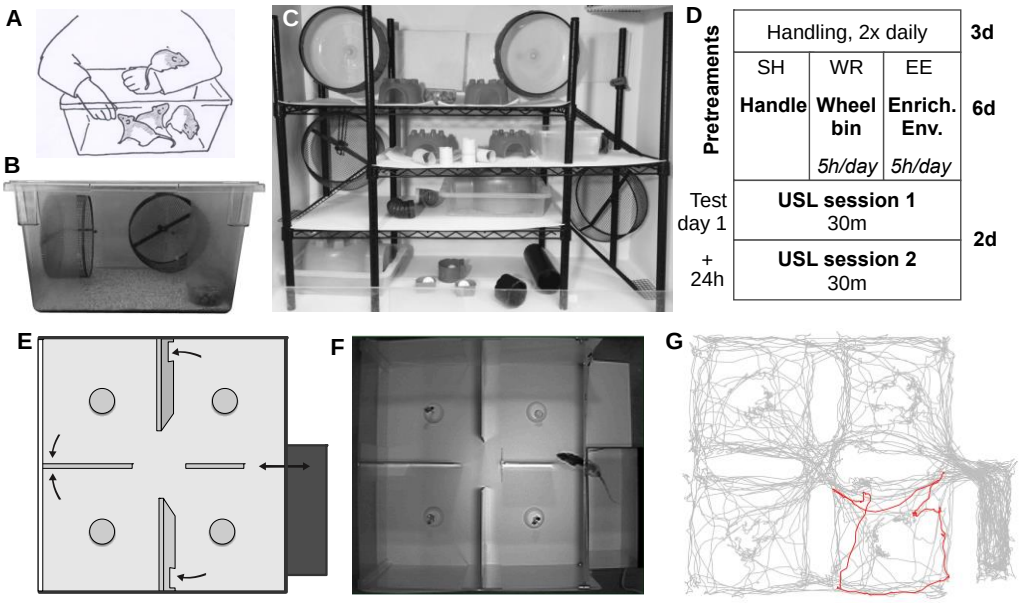


**Figure 3-1 Pretreatments and behavioral testing**

(A) Illustration of standard handling procedure at rat home cage. (B) Wheel-running bins. (C) The enriched environment, approximately 40x the volume of a standard rat home cage, included internal complexity with different levels and objects. (D) Schedule of pretreatments and behavioral tests by days (d). (E) Diagram of complex unsupervised learning arena (USL), showing 4 rooms, passageways, 4 distinct objects, and attached refuge. Each room may be accessed by at least three different routes. Distant visual cues (not shown) were visible from the arena. (F) Overhead camera view, with rat entering the arena; the rat is visible within the refuge only to the infrared-equipped camera. (G) Representative 30m trajectory, with the rat's first foray made into the complex arena shown in red.

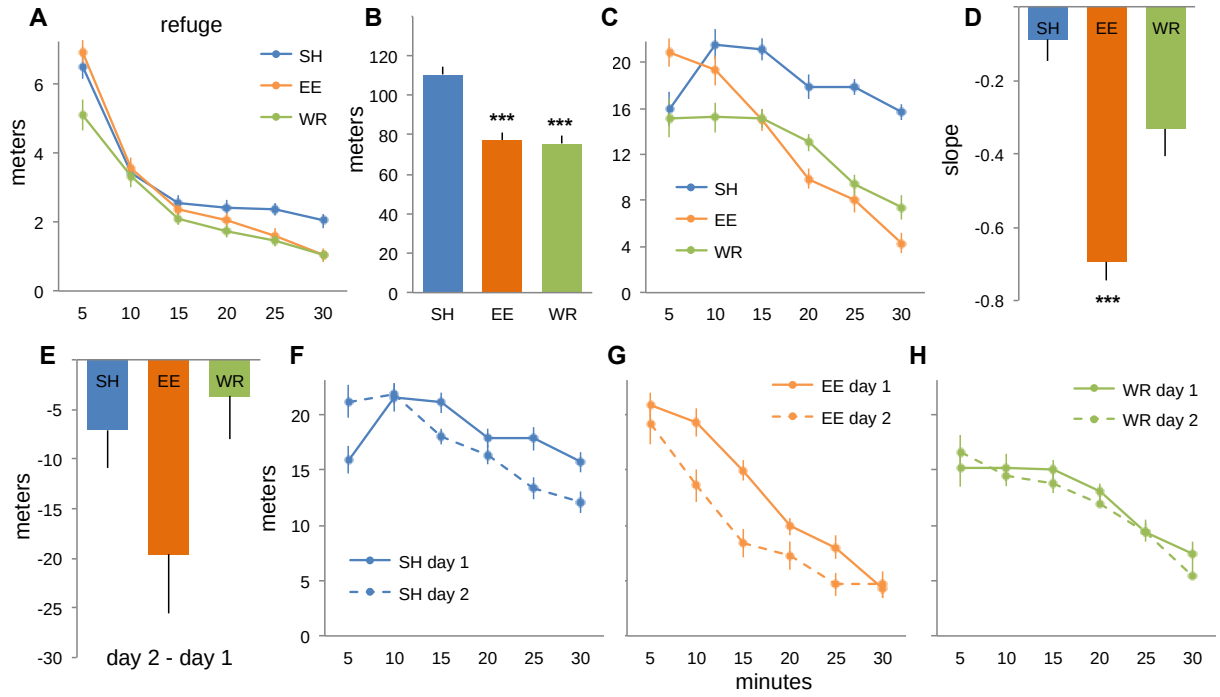


**Figure 3-2 Enrichment accelerated habituation in the complex arena: short and long term memory.**

Panels A-D show measures for the first session; E-H show changes in the second session given 24h later. (A) Distance travelled in the refuge during the first session is shown in six 5 min time intervals: all groups showed robust habituation in this simple environment. (B) Total distance traveled in the complex arena during the first session was greater for SH rats than the other groups (ANOVA: $p<0.0001$, SH vs. EE or WR; $p<0.0001$ on Tukey post-hoc tests). (C) Plots of distance traveled in 5 min time intervals in the arena on the first session show an effectively flat habituation curve for SH rats; WR rats display some habituation, and EE rats exhibit a much steeper habituation curve than the other groups. (D) Slopes of curves in panel C show the rate of habituation is greater for EE than SH or WR rats (ANOVA: $p<0.0001$, SH vs. EE or WR; $p<0.001$ on Tukey post-hoc tests). (E) The change from day 1 to day 2 in the total distance traveled in the arena was < 10% for SH rats ($p=0.08$, paired t-test day 1 vs day 2), while this drop was about 30% for EE rats across the two days ($p=0.002$, paired t-test), and unchanged for WR rats. (F) SH rats showed an only slightly steeper habituation curve in the complex arena on session two ($p=0.02$, paired t-test). (G) The EE group curve for the second day showed a steep drop from the first to the second time bin ($p=0.0003$, paired t-test), thus shifting the entire curve downwards relative to the first day. (H) WR group curves did not change between test days. (***) $P<0.001$.

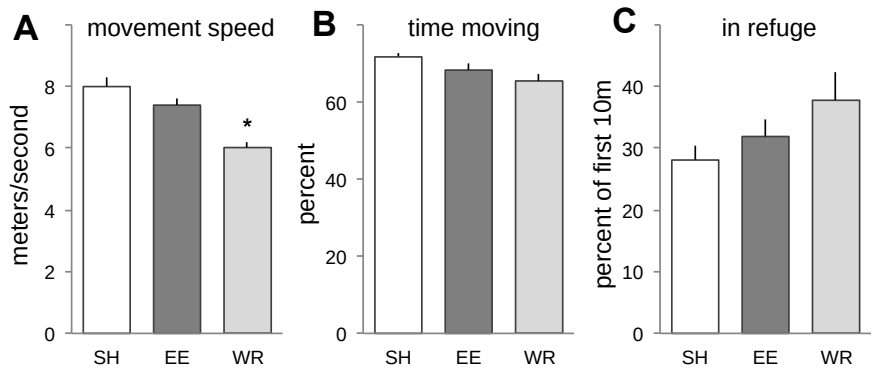


**Figure 3-3 Little to no evident difference in measures of arousal and anxiety**
(A) Speed of movements in the arena during the first session. Unexpectedly, WR group rats showed a small drop in average movement speed. SH and EE rats were not different. (B) Another measure of arousal, percent time moving while in the arena, was similar between the groups. (C) Percent of the first 10 minutes of the session that was spsent in the refuge; groups did not differ significantly on this measure. (*) $p < 0.01$. Additionally, the (empty, refuge-less) open field test was originally introduced by Hall to measure anxiety, primarily via quantification of defecations which, in rat, also serves as a conventional measure of anxiety or fearfulness; in our studies, likely in part due to the presence of the refuge and extensive handling, these counts were very low: usually none, with no group differences (data not shown).

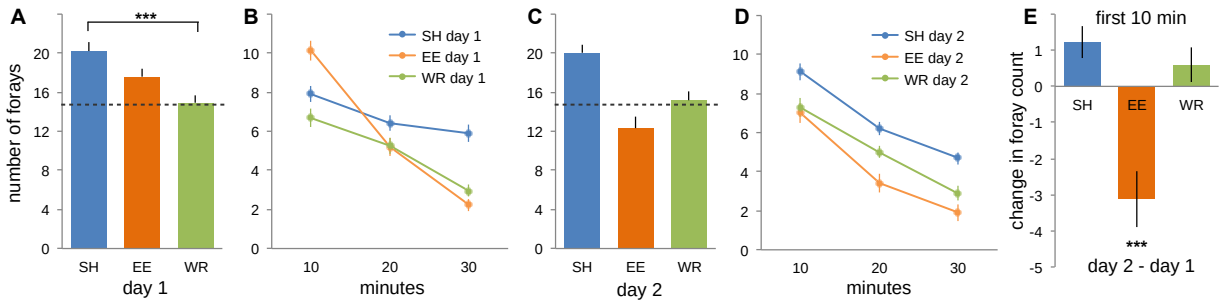


**Figure 3-4 Number and timing of exploratory forays are influenced by prior enrichment**
(A) SH rats made more forays during the first test session (day 1) than did WR rats (p=0.0002, ANOVA; SH vs. WR: p<0.001; other post-hoc comparisons were not significant). (B) EE rats began the session with a high foray count which halved in each successive 10-minute interval; changes in foray counts for SH and WR rats were more modest, with the slope of the EE curve much steeper than the other groups' (p<0.0001, ANOVA; EE vs SH or WR: p<0.0001; SH vs. WR: not significant). (C) Plot of day 2 foray counts show that EE rats markedly decreased total number of forays relative to 24 h earlier (P<0.0005, paired t-test) whereas SH and WR rats were unchanged (dotted line) (P<0.0005, paired t-test). (D) Foray starts in 10 minute bins on day 2. (E) Change in foray counts during the first 10 min of session 1 vs first 10m of session 2 dropped sharply for EE rats but not WR or SH rats (p<0.0001, ANOVA; EE vs. SH or WR, p<0.001). (***) P<0.001.

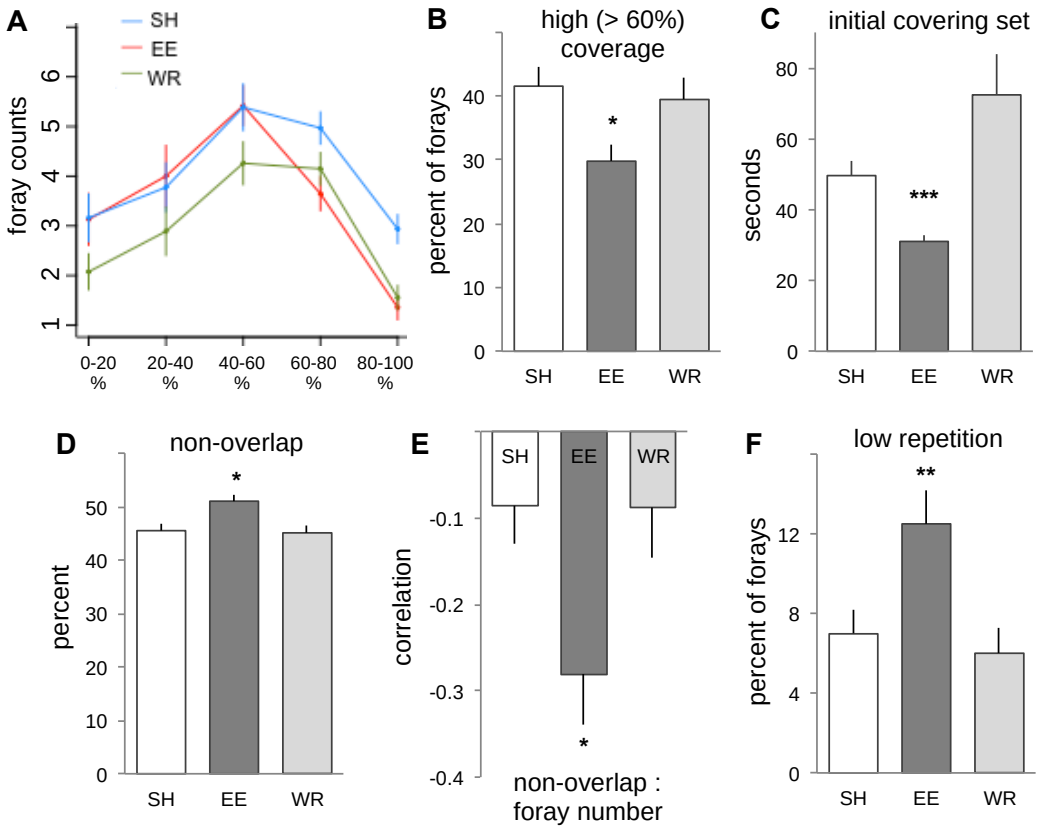


**Figure 3-5 Patterns of exploration in the novel complex arena are affected by prior enrichment**

(A) Percent of the arena covered by each foray is plotted in bins of 20% arena coverage. The curve for EE rats is left shifted, away from high-coverage forays, compared to SH rats; WR rats made fewer forays overall but with a similar distribution to SH rats. (B) The percent of high-coverage forays (> 60% of the arena) was lower for EE rats than for other groups (p=0.01, Kruskal-Wallace rank sum test, p<0.01 and p<0.04 for EE vs SH and WR respectively; SH and WR not different). (C) The average duration of the "initial covering set" of forays first used to attain full arena coverage (at least 90% of arena visited) was significantly shorter for EE group rats (p<0.0001, ANOVA; in post-hoc comparisons EE vs SH p<0.002, EE vs WR p<0.0001, SH vs WR p=0.06). (D) Plot shows the percent of each foray not visited in the immediately prior foray: EE rats had a small but significant increase in non-overlap of successive forays compared to the other groups (p=0.003, ANOVA, post-hoc tests p=0.009 and 0.007 against SH and WR). (E) The non-overlap measure was negatively correlated with foray number for EE rats (Pearson correlation coefficient; p=0.02, ANOVA, EE vs SH p<0.04, vs WR p <0.05). (F) Percent of forays with low repetition (> 75% of line crossings were unique) was greater for EE rats than for other groups (p<0.003 ANOVA; EE vs. SH: p =0.01; EE vs. WR: p<0.01; SH vs. WR: not significant). (*) P<0.05, (**) P<=0.01, (***) P<=0.001.

# Chapter 4 Locus of Encoding Sites Used during Acquisition of Episodic-like Memory

The neurobiological substrates for transfer from unsupervised learning to current conditions, as discussed in Chapter Three, have largely been a matter of conjecture. One widely discussed proposal holds that the earlier experience leads to the construction of anatomical networks that promote subsequent encoding (Tse et al., 2011); this idea stems from the observation that weeks or longer interactions in an enriched environment leads to the growth of dendritic branches and spines in the hippocampus and cortex in rodents (Globus et al., 1973; Greenough et al., 1973; Leggio et al., 2005; van Praag et al., 2000). However, the immense capacity of memory presents difficulties for this hypothesis: experiential learning in complex circumstances is a routine event in humans and animals outside the laboratory and it seems likely that growth would quickly encounter limits. We investigated this question by conducting the first detailed analysis of synapse numbers in hippocampus in rats that did or did not have several days of experience with an enriched environment.

An alternative to the dendritic growth hypothesis is that modifications to existing synapses involving LTP are used to encode effective acquisition strategies and relevant domain information during the enrichment period, and that these are sufficiently flexible to be applied in novel circumstances (see above). In support of this possibility, modeling work on hippocampal networks using empirically derived LTP induction rules, which do not involve new growth, found that memory capacity scales linearly with neuron number (Granger et al., 1994) and thus provides good evidence for sufficient capacity in mammalian brains. Related to these points is the question of *how* previously acquired strategies facilitate subsequent encoding. In the present case, transferred search patterns or exploratory behaviors could allow enriched environment (EE) animals to more effectively (more quickly and/or robustly) learn the many and diverse features of the new complex environment. This would be expected to produce greater

evidence for LTP in each of the intra-hippocampal connections associated with these characteristics. The present studies constitute a first test of the prediction that past enrichment increases the number of synapses expressing an LTP marker after exploration in a different complex context. Results confirmed this prediction, but the regional distribution of these changes was surprising.

**4-1. Effect of past experience with complexity on synapse numbers in hippocampus.**

We explored this idea that past interactions with an enriched environment increases connectivity in hippocampus so as to promote future learning by counting the number of synapses, labeled with an antibody against the synapse scaffold protein PSD-95, in nine anatomical hippocampal subdivisions. There were no evident differences between EE vs. Standard Housed (SH) rats in the number or size of contacts. Rats were sacrificed at the conclusion of a first 30-minute session in the test apparatus, during which the learning differences between EE and SH rats described above were replicated (not shown), and brain tissue sections collected and processed for immunofluorescence microscopy using antibodies against PSD-95, a protein that is uniformly distributed across post-synaptic densities at excitatory (glutamatergic) contacts (Petersen et al., 2003; Sassoé-Pognetto et al., 2003; Valtschanoff et al., 2001) (**Fig 4-1A**). Automated counting and measurement systems (see Methods) were used to collect synaptic data from nine dendritic sample zones in a cross section from the rostral hippocampus (**Fig 4-1B**). Mean counts of synapses across the measured hippocampal subfields were not greater in the enriched group **(Fig 4-1C**).

Synapse size is another variable that relates to communication within hippocampal networks because it correlates with the number of AMPA-type glutamate receptors attached to them (L. Y. Chen et al., 2007); the size of the AMPA receptor pool dictates the size of the EPSC elicited by a release event and thus relates to the potency of individual contacts. We used 3-D reconstruction technology to estimate the volume of the tens of thousands of immunostained

synapses found within a sampling field. The frequency distribution for sizes (percent of all contacts that fall into graduated size bins) was described by a Poisson curve, as described for EM measurements (Harris et al., 1992), and was not detectably different between SH and EE brains for each of the hippocampal subfields measured (**Fig 4-1D**, p=0.09). Next, we measured the density of PSD95 protein at clusters matching the size constraints of synapses. There were no evident differences between SH and EE animals in comparisons of the nine subfields (**Fig 4-1F**, p=0.24).

We conclude from these results that six days of experience with a very complex environment does not produce lasting changes to the numbers, size, or structure of hippocampal synapses.

## 4-2. Effects of episodic-like learning on overall changes in the density of an LTP marker.

We tested for the induction of a synaptic marker for LTP during the first session in the novel complex arena. Studies on hippocampal slices showed that LTP consolidation requires activation of a complex array of signaling cascades leading to the formation and subsequent stabilization of actin networks in dendritic spines (L. Y. Chen et al., 2007). Phosphorylation (inactivation) of the actin severing protein cofilin is a critical step in the actin polymerization phase of this process (Rex, Chen, et al., 2009). Rats were sacrificed at the conclusion of a first 30-minute session in the arena, during which the above described learning differences between EE and SH rats were replicated (not shown), and 4-5 sections collected from the rostral hippocampus. These were processed for dual immunostaining of PSD-95 and phosphorylated (p) cofilin (**Fig 4-2A**) as described in previous work cited above. The percentage of contacts with dense concentrations of pCofilin was measured for 66 contiguous sampling zones that covered apical and basal dendritic fields of CA1, CA3, and dentate gyrus in an entire cross section (**Fig 4-2B**). Comparisons were thus made between rats (EE group) that rapidly learned during the session vs. animals that did not (SH group), although both groups explored the space to about

the same degree. We began the analysis with ten primary anatomical divisions of the hippocampal dendrites (see above). The total number of pCofilin immuno-positive contacts was the same for the two groups (SH: 0.73 ± 0.05 million/rat; EE: 0.75 ± 0.04; **Fig 4-2C**). Moreover, the mean number of double-labeled synapses was comparable for the two groups across each of the eleven zones (**Fig 4-2D**). Note that absolute values differed between zones and were well correlated between SH and EE groups (r=0.995). The relatively low variance and high degree of correlation indicates that the same regions were reliably outlined between sections, animals, and groups.

We then tested if the percentage of synapses co-localized with high concentrations of pCofilin was detectably different between the two groups in averages for all eleven sampling fields covering an entire cross section of hippocampus. Frequency distributions (percent of double labeled contacts vs. density of pCofilin) were constructed by averaging the distributions for the animals for each region. The resultant curves for the two cohorts of SH rats did not perfectly align and a comparable shift between cohorts was seen in the EE group (**Fig 4-2E**). We therefore compared the SH vs. EE frequency distributions separately for each cohort. The curves for the EE rats were slightly skewed to the right (higher densities) in each cohort relative to those for the SH group (2-way RM- ANOVA: $p<0.0001$ in each case), indicating that the former had a small but reliable increase in synapses with high levels of phosphorylated cofilin. The slight differences in the shape of the frequency curves for the two cohorts argued against combining them into a composite curve for either the SH or EE groups. We therefore subtracted the mean SH curve in a cohort from each animal (SH and EE) in that cohort, thereby creating a difference from control curve for individual rats. The difference curves were then combined for the two cohorts. The results indicate that the EE animals progressively deviated from the SHs across higher density bins ($p<0.0001$; **Fig 4-2F)**, in agreement with the rightward skew seen in the frequency distributions for each cohort. These results establish that effective learning of a complex arena by rats having prior experience with complexity is accompanied by a small

overall increase in contacts associated with an LTP marker, compared to rats without such experience that did not display behavioral evidence of learning.

**4-3. Regionally differentiated effects of episodic like learning.**

Next, we asked if the group effects described above reflect a uniform increase in phospho-Cofilin density at synapses across the hippocampus as opposed to regionally differentiated effects. Difference curves of the type described in figure 5F were accordingly calculated for each of the eleven hippocampal subfields (Fig 4-3; dentate gyrus polymorphic zone not shown). Striking regional effects were found: the stratum oriens and stratum radiatum of field CA1 both had steeply rising curves reaching values that were double the baseline (SH) scores (**Fig 4-3A**). Labeling in the lacunosum-moleculare lamina of CA1 was also increased as was the stratum oriens of field CA3c. There were no statistically significant effects in any of the remaining divisions. The increases in densely labeled synapses (≥ density bin 135) for field CA1 in EE relative to SH rats involved only a small percentage of the entire population (CA1 stratum oriens: SH = 1.14 ± 0.15% of the population; EE = 1.98 ± 0.23%; p=0.009, t-test). Thus, the largest regional effect associated with rapid learning involved an approximately 1.0% increase in densely labeled contacts. Changes across the entire cross section, including regions in which group differences were barely detectable, would necessarily be much smaller than this value. In all, it appears that the stable encoding of a large amount of information by EE rats during a 30-minute session in a novel, complex environment is associated with a very economical use of storage elements.

To facilitate comparisons between regions, we calculated the slopes for the difference curves for density bins 90-185 for each of the EE rats. This analysis confirmed that the basal and proximal apical dendrites contained higher percentages of synapses with dense concentrations of pCofilin than the remainder of the hippocampus (**Fig 4-3B**). As seen in the error bars in the previous figure (i.e. **Fig 4-2 panels A,B**) there was considerable variability

between individual rats in the EE group. We therefore normalized the regional values for each animal to its mean for all zones, a step that eliminates any between-animal differences in slopes. The results confirmed that the two CA1 fields had a much higher percentage of synapses associated with high concentrations of pCofilin relative to SH rats than found in the nine remaining zones (**Fig 4-3C**).

Fine grained analyses of regional effects. The results for large sampling fields establish that LTP related synaptic effects in the hippocampus of EE animals are largely restricted to two subdivisions of field CA1. The question then arises of whether further differentiation can be detected with finer grained analyses. We used 66 contiguous sampling fields and the slopes for differences between the positive tails of the frequency distributions to test the point. As expected, the within group variability was high for this analysis but there was a clear regional effect in the EE group (**Fig 4-4A**). There were eight zones in which the mean slope in the EE group was ≥1.5 (dotted line) but only two of these (CA1-stratum radiatum 3 and 4) were statistically different in post-hoc tests ($p<0.05$, Tukey tests) from the corresponding SH areas **(Fig 4-4A**). One of the EE rats had a mean slope value for all fields that was 3.2 SDs lower than the mean value for the remaining rats. Excluding this case, increased the statistical difference between the distributions for EE vs. SH groups and added post hoc differences for CA1 stratum oriens 3&4 ($p<0.01$).

Normalizing the regional values for each of the eleven animals to its mean for all 66 zones, to reduce within group differences, confirmed that marked regional distributions of slope values were present within the EE group (**Fig 4-4B**). Excluding the one case noted above again extended the difference from other regions in the EE group to CA1 SO 3&4 in post hoc tests ($p<0.01$).

It is noteworthy that 5 of the 8 areas with the greatest differences from controls were located in the same medio-lateral region of field CA1 (lateral CA1a and medial CA1b; **Fig 4-4C**). A clustering score was calculated for each rat by comparing the mean values for the eight sites

vs. the remaining 58 zones. There was considerable variability within the EE group but clear differences were present for each animal: the mean slope (normalized; Panel B) for the target fields was 1.17 ± 0.23 and -0.16 ± 0.03 for the remainder (p=0.00001, **Fig 4-4D**). Having a single value for each rat made it possible to test for a predicted correlation between learning (initial habituation rate) and pCofilin cluster score. This did not reach statistical significance for the entire group (Spearman r = 0.43, one tail p=0.096) in large part because of an animal that was much less active during the session than the other members of the group, which varied only slightly (49.7 meters vs. 100.1 ± 4.9 meters). Excluding this case resulted in a robust correlation (r= 0.72, p=0.012).

**4-4. Distribution of encoding sites engaged by a simple form of unsupervised learning.**

The above results can be compared to those obtained from rats that learned a very simple environment and without prior experience with complexity. Adult, male rats were divided into three treatment groups: 'contingency' (n=8), unsupervised exploration (n=8), and home cage controls (n=7). All rats were handled twice daily for 6 days, and on the following day were given behavioral testing or left in home cages. The testing apparatus (36 x 18 x 18 inches in length, width, and height) was divided into two equal-sized compartments distinguished by either black-and-white stripes or square dots on one wall, with a 4 square inch connecting passage; one compartment had a strobe light (3W LED) and a toy siren alarm fixed above (**Fig 4-5**). Rats in the contingency group were placed into the apparatus and allowed 5 min of exploration, after which any further entries into the 'strobe' compartment activated the strobe light and alarm as long as the animal remained there; this strobe contingency period lasted 25 min. Rats in the unsupervised learning group were given 30 min to explore the compartments with no strobe or alarm activation. Home cage controls did not have behavioral testing. On removal from the test apparatus (or home cage), each rat was anesthetized and their brains removed and fast frozen for later immunofluorescence. In all, one group was allowed free

exploration of a simple space while the other was prevented from doing so: unsupervised episodic elements were minimal and there was no opportunity to employ search strategies in the small space.

The free exploration rats distributed their time equally between the two compartments (**Fig 4-6A**), while the rats exposed to the sound / light avoided the pertinent room (**Fig 4-6B**). This pattern was observed for each of the eight rats in the two groups (**Fig 4-6B**). Importantly, the contingency animals periodically triggered the signals with short moves into the room throughout the trial (not shown). Exploratory activity, as assessed by total distance traveled during the session, tended to be slightly lower in the contingency group (63.9 ± 9.4 meters) than in the unsupervised group (79.6 ± 7.8) but this difference did not approach statistical significance ($p>0.20$; 2-tailed t-test). Reductions in activity over time in the test chamber (habituation), a measure of short term memory, occurred at similar rates in the two groups: the mean of the individual slopes for the exploration group was -0.56 ± -0.05 while the corresponding values for the contingency animals were -0.55 ± -0.08 ($p>0.76$) (**Fig 4-6D**), a result suggesting that stress and arousal levels were not greatly different between groups.

We ran additional groups (n=8) to test if 30 minutes of experience sufficed to produce long-term memory in unsupervised, free exploration rats. Habituation and overall activity on day one were comparable to that in the day one group used for synaptic mapping. However, day two activity was greatly reduced relative to day one ($p<0.0001$, two way ANOVA for group effects) and, on day two, the rate of habituation was accelerated ($p=0.028$) (**Fig 4-6E**). There was no difference in overall activity or habituation rates between days one and two for the rats in the contingency group (Fig 4-6F); note that these animals experienced a change in the environment on day two, namely, no aversive cues on the second day.

Sections were stained as above with PSD-95 and another marker of LTP, phosphorylated CaMKII$\alpha$ (**Fig 4-7A**), and digital images collected. To evaluate the regional distribution of the LTP marker at synapses, the hippocampal image was divided into 42 zones

that conformed to local cytoarchitectonic and laminar boundaries (**Fig. 4-7B**). We then subtracted the 'hot spot' score, a thresholded z-score, for the home cage group from the values determined for individual unsupervised exploration and contingency rats. The mean of all positive values was greater in the exploration group than in the contingency group ($p=0.03$). Clear differences between the home cage and contingency groups (one SD greater than the mean for all positive sites) were absent. However, four regions meeting this criterion were present in the exploration group (**Fig 4-7C**). Three zones in the unsupervised exploration group (stars, **Fig 4-7C**) differed from two or more other zones in that same group by $p<0.001$ in post-hoc tests after one-way ANOVA. There were no zones of this type in the contingency group. We interpret these results as indicating that unsupervised learning of an open field causes large LTP-related synaptic changes in a surprisingly small number of sites, and that this does not occur if behavior is channeled by the introduction of a response contingency.

In all, the maps generated in a simple, non-episodic context are very sparse (few hot spots) and bear no resemblance to those described earlier. These maps, especially those related to the episodic task constitute evidence that focal sites of memory storage emerge in the CA1 during episodic learning. Initially this would seem to contradict the previous modelling results. However, pCofilin is an extremely short-lived protein, previous studies have shown it peaks around 2-7 minutes and has declined by 15 minutes. (L. Y. Chen et al., 2007). EE animals appear to be performing their maximal exploration during the first 5 minutes but explored for 30 minutes. It's possible that the sites represented here are actually sites of some sort of consolidation and not of the initial storage. It is also possible that the amount of synapses required for temporal storage in the CA3 is broad and requires a small population of cells, less than would be detectable for our system, while storage in the CA1 uses a (relatively, still less than 1%) large number of focal synapses.

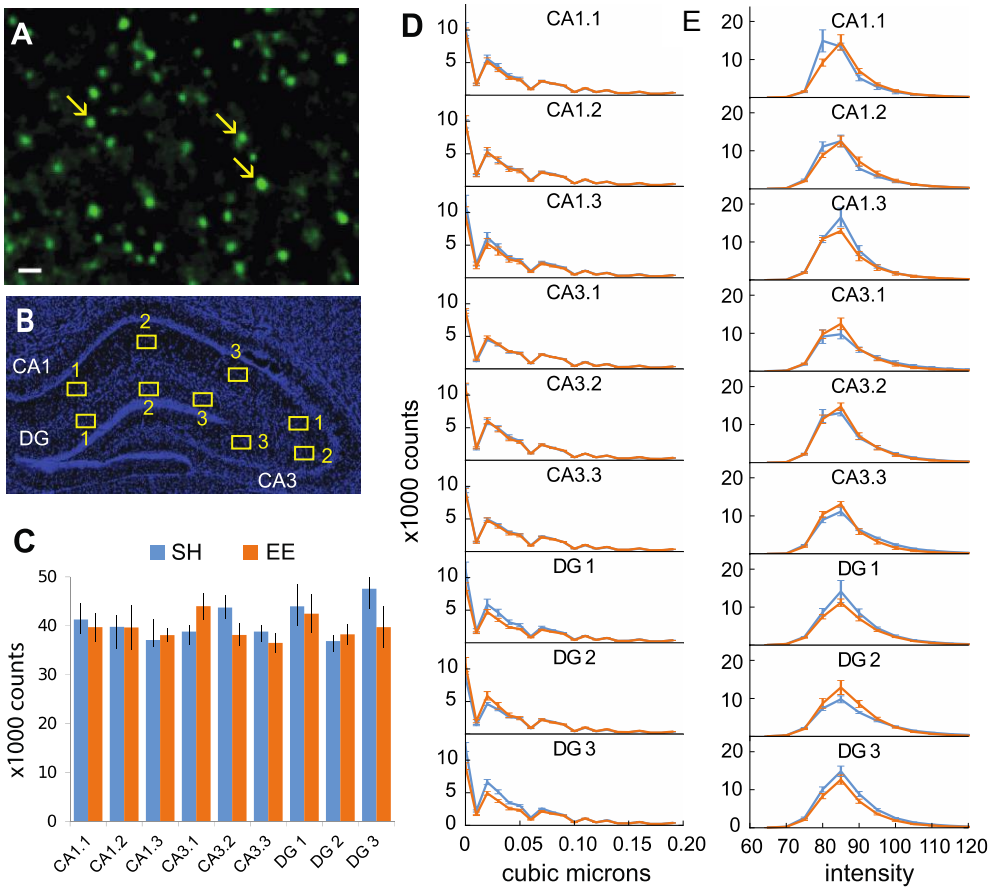


**Figure 4-1 Synapse counts are not different between groups**
(A) Representative image showing PSD95 immunoreactivity; arrows indicate example puncta. (B) Illustration of sampling zones in each of dendritic fields of CA1, CA3, and dentate gyrus. (C) Mean synapse counts for each subfield sampled were not different between the enriched and standard handled groups (p=0.44, 2-way RM-ANOVA). (D) Frequency distribution (percent of all synaptic puncta falling into size bins) for each of the nine subfields. There were no differences in size measurements between the two groups (p=0.09, 2-way ANOVA). (E) Frequency distributions for labeling density for each subfield. There were no differences between the two groups (p=0.24, 2-way ANOVA).

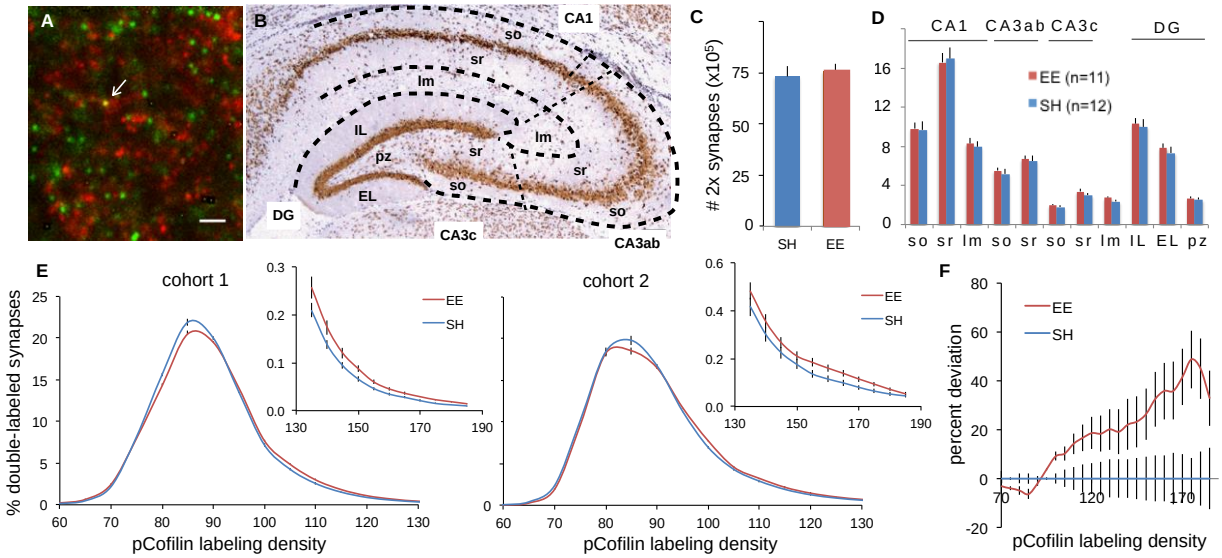


**Figure 4-2 Synaptic pCofilin levels show consistent regional measures with enriched rats displaying an increase in high density pCofilin labeling after learning in a novel complex environment**

(A) Representative deconvolved image shows dual immunolabeling for PSD95 (green) and pCofilin (red); arrow indicates double labeling (yellow). Scale bar = 2μm. (B) Diagram illustrating the eleven dendritic zones measured, including CA1 stratum oriens (so), stratum radiatum (sr), and lacunosum moleculare (lm); field CA3ab (so, sr); field CA3c (so, sr), CA3 lm, the dentate gyrus (DG) molecular layer internal leaf (IL) and external leaf (EL), and the polymorphic zone (pz) of the dentate gyrus hilus. (C) Total counts of double-labeled puncta across all zones were comparable for SH ($0.73 \pm 0.05 \times 10^6$) and EE ($0.75 \pm 0.04 \times 10^6$) rats (p=0.44, 2-way RM-ANOVA). (D) Counts of double-labeled synapses in each of the eleven zones were similar and well correlated (r=0.995) between EE and SH groups. (E) Immunolabeling frequency distributions for all zones combined (plots show the percent of double labeled contacts in different pCofilin immunolabeling density bins) for the animals in each group, shown for each of the two cohorts. A shift between cohorts was apparent in both groups; frequency distributions were therefore compared separately for each cohort. Insets: comparison of the right tail (higher densities) for each cohort reveals a small but consistent increase in synapses with higher levels of pCofilin for EE compared to SH rats (2-way RM-ANOVA: P<0.0001 for each cohort). (F) Mean difference from within-cohort SH curve (mean SH curve for a cohort subtracted from the curve for each rat from either group in that cohort). EE group rats' deviation from SH mean increases with higher density bins (P<0.0001), in accordance with the rightward skew of the frequency distributions.

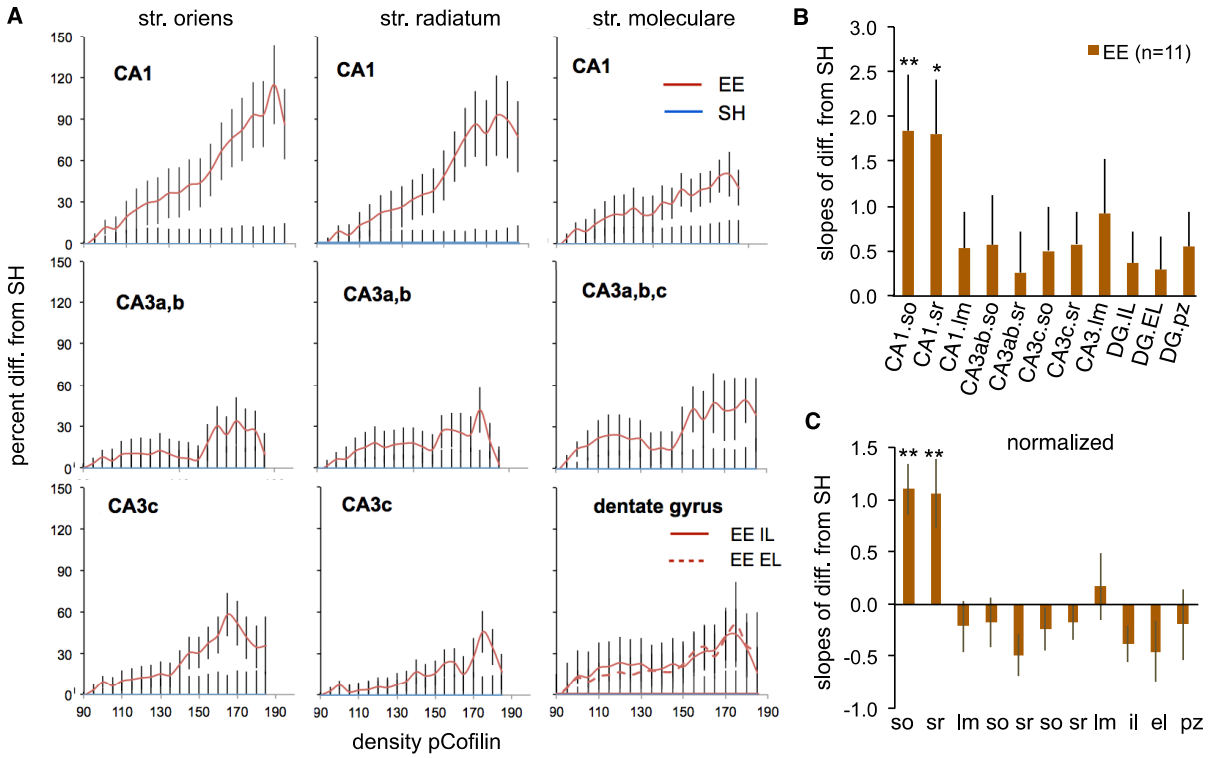


**Figure 4-3 Synapses with dense concentrations of synaptic pCofilin are concentrated in field CA1 in animals with past experience with complexity**

(A) Percent difference (y-axis) from the positive tail of the mean frequency distribution curve for SH rats (x-axis: successively higher pCofilin density bins); results are summarized for 10 of the 11 hippocampal subfields (polymorphic zone of hilus (pz) not shown). Orange lines show average values for 11 EE rats in each panel; average values for the 12 SH rats (blue line) is included here to show between-animal variability. Curves for CA1 stratum oriens (str. oriens, so) and stratum radiatum (str. radiatum, sr) progressively increased in the EE group across 16 density bins shown, indicating that the frequency distribution curves for these two areas were strongly right shifted from the corresponding zones in the SH group (2-way RM-ANOVA, $P<0.0001$ in each case). CA1 lacunosum moleculare (str. moleculare, lm) and CA3c-so were also increased ($P=0.002$ and $P=0.0016$ respectively); there were no other significant effects. (B) The slopes of the difference curve from the mean of the SH group were calculated for each region in the EE rats to provide a single value for comparisons between regions within the EE group; there was a clear regional effect (RM-ANOVA: $P=0.008$) with CA1-so ($P=0.005$,Tukey test) and CA1-sr ($P<0.03$) increased above other areas. (C) Normalization of regional values for each EE animal to its mean (all regions) difference from SH rats confirm that CA1-so and -sr have a higher percentage of high-concentration pCofilin synapses than the other zones (RM-ANOVA: $P<0.0001$; CA1-so: $P=0.002$; CA1-sr: $P=0.002$; Tukey tests). Additional abbreviations: DG, dentate gyrus; IL, internal leaf; EL, external leaf.

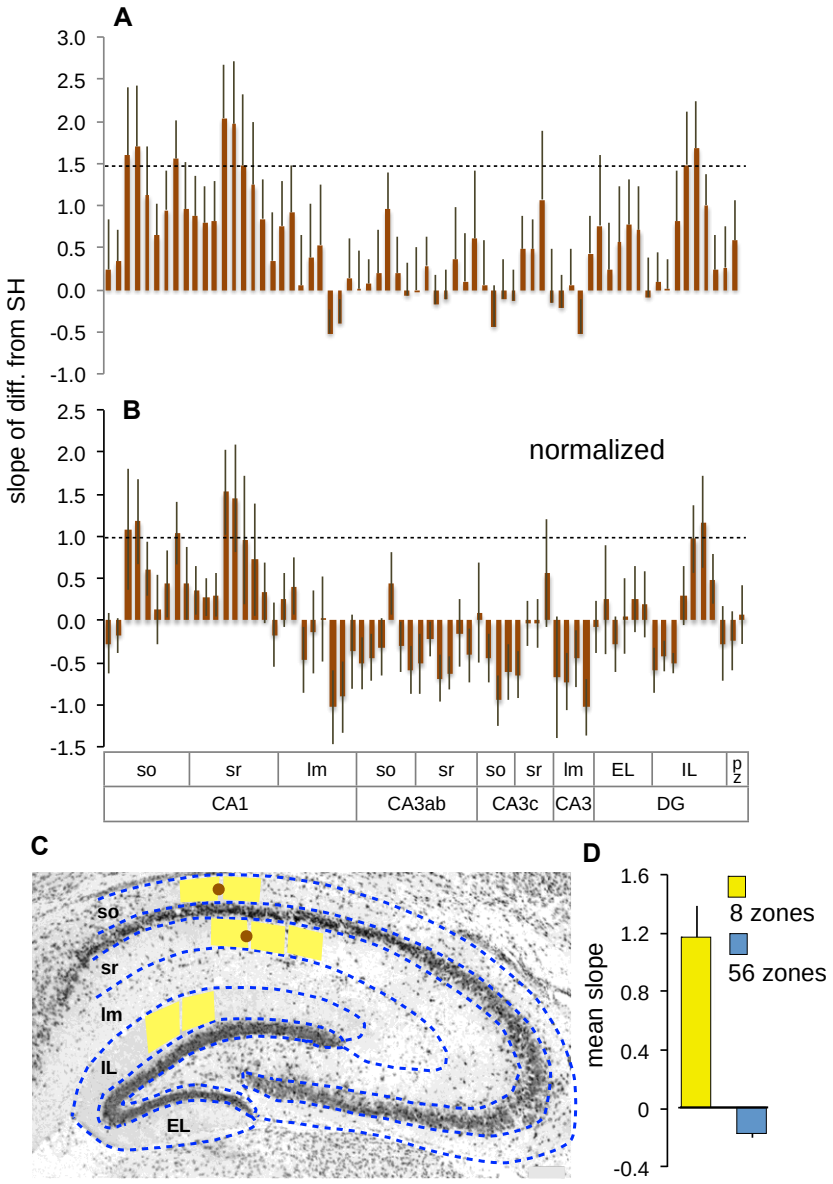


**Figure 4-4 Division of the eleven original sampling regions above into 66 contiguous subsampling zones reveals hot spots and clustering effects in EE group**

(A) Slopes of EE vs. SH differences across increasing pCofilin density bins (see text) were calculated for 66 fields. Regional distribution of differences from SH frequency distribution curves were significant (two-way RM-ANOVA, P=0.0005). Two subzones, CA1-sr 4 and 5, differed in post-hoc Tukey tests (P=0.03, 0.04). (B) Regional values for each animal in the EE group were normalized to the mean score for that animal for all 66 sampling areas; there was a strong regional effect (one way ANOVA: P<0.0001) with CA1-sr 4,5 different from other areas in post-hoc tests. (C) Locations of eight subfields where mean EE slopes were ≥1.5. Notably, CA1 'hotspots' were located in adjacent basal and apical dendrites (brown dots). (D) The mean values for the eight areas were calculated and compared to the means for the remaining 58 areas for each EE rat to provide a measure of relative clustering. The group difference for the two collections of sampling fields was significant (P=0.00001, t-test).

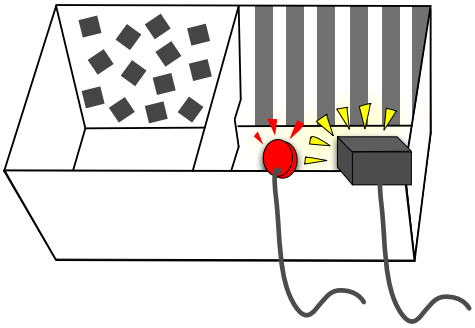

**Figure 4-5 Diagram of strobe-alarm apparatus**
Under the strobe-alarm contingency condition, overhead video camera tracking triggers the strobe light and alarm sound whenever the rat enters the room at right, and shuts off if the animal leaves the room.

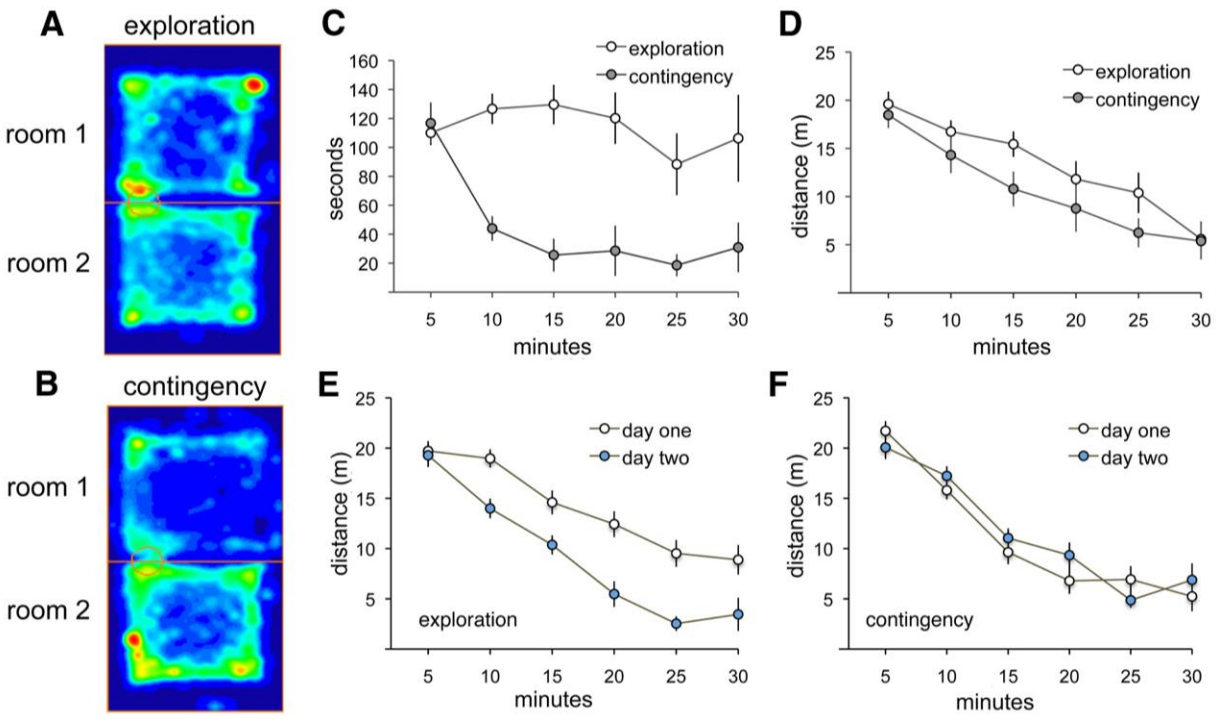


**Figure 4-6 Behavioral analyses demonstrate differences in exploratory behavior between experimental groups**

One group (contingency) explored freely for 5 min, after which entry into one compartment (Room 1) triggered a flashing light and a buzzer over the remaining 25 min; the second (unsupervised "exploration") group was allowed explore both rooms with no contingencies for 30 min. (A), (B) Heat maps show the time spent at different locations over 30 min in the two compartments by representative rats from each group (red > yellow > green > blue). (C) Quantification of time spent in Room 1 for each group, in 5 min time segments over the 30 min session (n = 8/group). Note the steep drop after minute 5 for the contingency group. (D) Distance traveled, in both compartments, by unsupervised "exploration" and response "contingency" groups demonstrates similar habituation curves. (E) Comparison of distance traveled per 5 min bin in a separate group (n = 8) of unsupervised exploration rats tested on 2 consecutive days. The between-day difference in these habituation curves was highly significant, as was the total distance traveled over 30 min ( p = 0.0001, 2-way ANOVA and t test respectively). (F) Same curves as in E but for contingency rats (n = 8; separate set from those in C and D); there were no detectable differences between days 1 and 2.

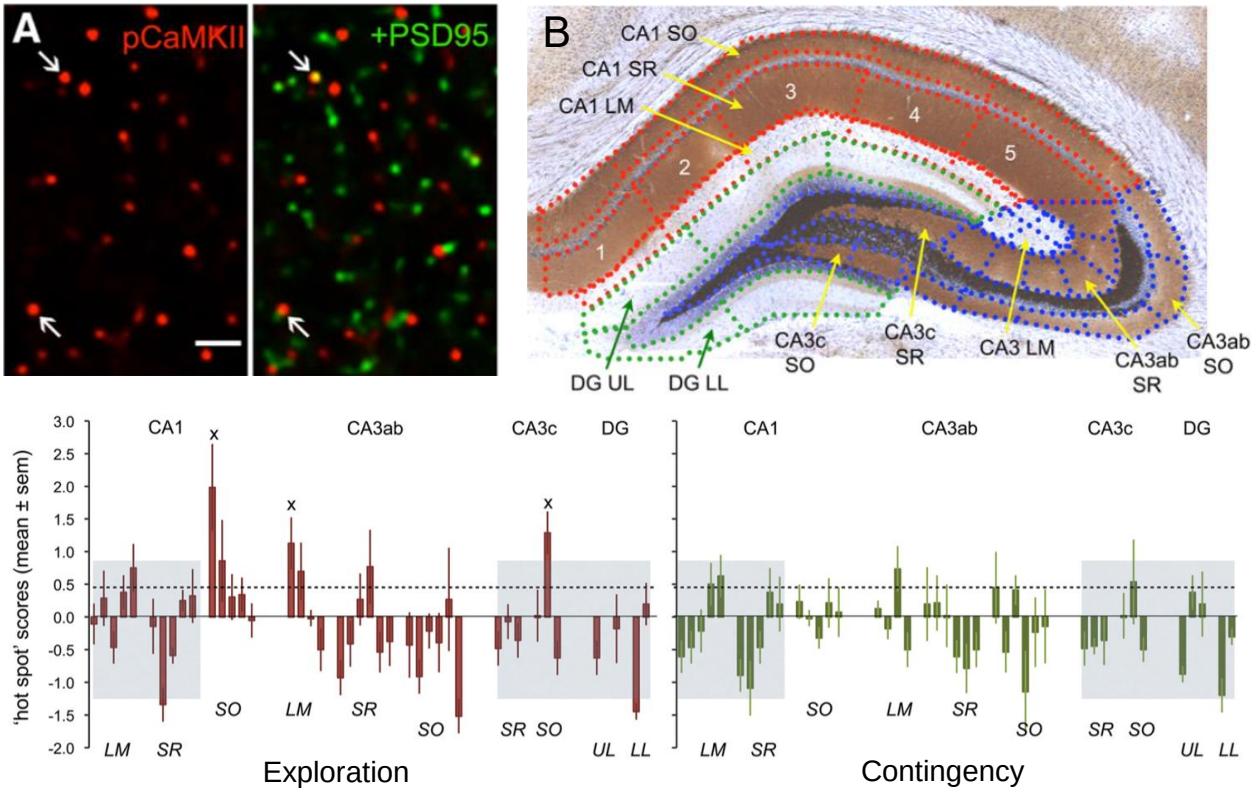


**Figure 4-7 Dual immunofluorescence localization of PSD95 and pCaMKII T286/287 was used to map colocalization across 42 sample zones in rostral hippocampus**

(A) Representative images show immunolabeling for pCaMKII alone (left, red), and for pCaMKII plus PSD-95 (right, red and green, respectively) in stratum radiatum (SR) of field CA1b. Scale bar, 2 micrometers. Note, both antigens are exclusively and densely localized to small puncta, some of which were double labeled (arrows, 2 examples of colocalization). (B) Photomicrograph of a rostral hippocampal section processed for the Timm's stain for heavy metals (brown to black) and Nissl staining (violet) to illuminate major lamina and cellular layers, respectively. Sampling zones used for automated counting of pCaMKII+ and PSD-95+ elements are indicated with dotted lines. Each of the major hippocampal subdivisions (CA1, CA3ab, CA3c, DG) were divided into 4 – 6 zones as illustrated for CA1 SR: these numbered zones (1–5) extended across the three lamina in fields CA1 and CA3. Numbering within CA3 and the DG molecular layer began with CA3a and the lateral aspect of the upper leaf, respectively. LM, Lacunosum-moleculare; SO, stratum oriens; UL, upper leaf of the DG molecular layer; LL, lower leaf of the DG molecular layer. (C) "Hot spot" scores for unsupervised Exploration (left) and Contingency (right) groups following subtraction of mean values from home-cage animals. The dotted line is the mean of positive values for the two groups and the height of the gray boxes is 1 SD above that mean. Subtracting home-cage scores reduced several strongly positive values in the exploration animals, mainly in stratum oriens (SO) of CA3a,b, thereby increasing the relative sizes of the remaining hot spots. The same subtraction procedure eliminated all values >=1 SD above the mean in the contingency group; despite this, the 21 sampling fields within the gray boxes were highly correlated with the corresponding sites in the unsupervised exploration group. The overall patterns were statistically different between the groups, particularly in the noncorrelated region between the gray boxes. The x's indicate three regions that were robustly different ( $p < 0.001$) than >=2 of the remaining sampling zones in the same Exploration group.

# Summary and Discussion

Converging lines of evidence indicate that the hippocampus is critical to the acquisition and retrieval of human episodic memory, a conclusion that aligns well with the broader idea that the structure plays a major role in a variety of species in the processing of sequential cues. But knowing that a brain region is involved in a given operation (its activity correlates with performance, silencing blocks function) does not explain the nature of its contribution. The hippocampal formation, as described in the literature, is part of a cortical-hippocampal-cortical loop that receives input from multiple association areas of cortex and then sends dense projections back to these regions (Kesner et al., 2015; Norman et al., 2003; Squire et al., 2004). The interconnected cortical portions of these 'loops' organize information along many dimensions including extended sequences and hierarchical categories. What then is the unique contribution of the hippocampus? One approach to this question is to ask if the region possesses features that are both logically related to the inferred computations and lacking in the remainder of the telencephalon. The dentate gyrus is certainly a striking example of the latter. This subdivision, often referred to as the gateway to hippocampus because it is the primary target of cortical input, is composed primarily of a peculiar type of neurons, the granule cells, whose only comparators are found in the olfactory bulb and cerebellum. The mossy fiber projections of the granule cells can only be described as bizarre: they innervate only a single region (field CA3 pyramidal neurons), via axon terminals of which most are enormous (Rebola et al., 2017). Moreover, the dentate gyrus-CA3 connection is extremely convergent: individual granule cells contact a very small number of CA3 neurons (tens to a few hundred) (Rolls, 2008). However, while satisfying the criterion of being unique to hippocampus, the dentate gyrus does not possess the type of neuron-to-neuron connections generally assumed to provide for associations between cues. Indeed, there are currently no formal hypotheses that relate the peculiar features of the region to any particular function.

In prior work we began to address the above question by comparing signal processing at mossy fiber synapses with that at six other steps in a network leading from input to olfactory (piriform) cortex through hippocampal field CA1. Responses to a 20 second train of theta stimulation, a dominant frequency for hippocampus, were measured at each node of the circuit. All steps leading to the dentate gyrus exhibited weak, steadily decaying facilitation while connections in the subsequent pyramidal cells had robust and sustained enhancement. In contrast to either of these patterns, the mossy fibers responded to theta input with a several-fold, sustained facilitation. We built a several stage simulation of this cortico-hippocampal network to evaluate the functional outcome from these markedly divergent frequency facilitation effects and found that the output of the network stabilizes at a high level in large part because of the unique behavior of mossy fiber synapses (**Fig 5-1**). In all, the singular characteristics of the dentate gyrus allow that region to serve as an amplifier that compensates for steadily decremental input from cortex (Trieu et al., 2015).

It is clear from the above that the hippocampus thus operates in a very different manner than cortex but this conclusion alone does not point to a special role in the processing of sequential information. This led us to a second unusual feature of the structure: the massive recurrent collateral projections within field CA3. As argued by a number of theorists, this system seems well suited for maintaining representations of transient input from cortex across extended intervals (Kesner et al., 2015). This would allow for linkages between spaced cues. As a first step in testing this idea, we first built a biophysically realistic network simulation, incorporating the very potent mossy fibers, to investigate this basic idea and found that it generated the sharp wave effect that is a characteristic marker of recurrent hippocampal activity in vivo. A more sophisticated model, constrained by a battery of anatomical and physiological CA3 features, maintained signals into the seconds range after a experiencing a brief input. Adding LTP based synaptic plasticity enabled linkages between temporally spaced cues. An analysis of parameter space in the model confirmed the expectation that the density of recurrent innervation is

essential for maintaining the activity initiated by a brief initiating signal. We conclude that this unique structure in hippocampus enables operations --- connecting widely spaced inputs --- that are beyond the capabilities of the weaker associational projections found in cortex. Importantly, initiation of cycling activity in CA3 was dependent on the mossy fibers, another factor absent in cortex.

Essential aspects of episodic memory unexpectedly emerged from the model. Presentation of a first cue in a sequence triggered representations of subsequent events and in the order in which they had been originally sampled. Still more surprising, retrieval of the cues was time compressed while maintaining relative delays between them. Analysis of the simulations confirmed that these phenomena were generated by those aspects of hippocampus not found in the cortical relationships. To the extent it has been studied, these aspects are common to the mammals and certain of them appear to have homologies in the other amniotic vertebrates (see (Striedter, 2016)). This suggests that aspects of episodic memory, including time compression during retrieval (Nádasdy et al., 1999), are emergent properties of designs shaped by early evolutionary pressures for less complex, time related operations. We conclude that the nature of the contribution made by hippocampus to the processing of sequential cues in small-brained rodents and episodic memory in humans i) arises from highly specialized features missing from cortex, and ii) involves associations over very long intervals associated with a compression of time.

The ratio between the size of neocortical association areas to that of hippocampus is orders of magnitude greater in humans than is the case for rodents. It follows that the manner in which the output of the latter is processed by the former will be vastly different; similarly, the type and complexity of information received by hippocampus is certain to be radically different between the two species. Therefore, while we can imagine that the operations performed by our model are common to rats and people, the phenomena generated by cortico-hippocampal-cortical loops are going to be qualitatively dissimilar. We accordingly expect that many aspects

of episodic memory as identified in a large literature on human work will at best be poorly expressed in commonly used laboratory animals. In all, we hypothesize that the dentate gyrus-CA3 system serves as a clocking device that is common to the mammals although producing distinct outcomes depending on the size and organization of its cortical relationships. Prior work showed that rodents encode the temporal order of cues but surprisingly there have been no direct tests of whether this is dependent on field CA3. The modeling studies suggested a means for executing such experiments involving transient silencing of the commissural component of the subfield's recurrent collateral system. As predicted, this manipulation entirely removed the ability of mice to remember the sequence in which odors had occurred while leaving intact the memory of cue identity.

Rodent work has to date focused on tests in which the basic 'what', 'where', and 'when' elements of an episode are studied in isolation. But these aspects occur together in real world circumstances and are incorporated into an integrated memory; the degree to which animals accomplish this routine human operation is unknown (Easton et al., 2012). Tests of this would minimally require assessing the contributions to behavior of hippocampal pathways associated with each element in paradigms involving discrete episodes of unsupervised exploration in a naturalistic environment. We developed a first test situation of this type by connecting a large complex arena with a much smaller, darkened side room; under these circumstances, rats explored the larger area using individual forays separated by periods in the attached 'refuge'. An intriguing complication with human relevance was immediately encountered: conventionally handled animals showed little evidence of learning during a 30-minute session. This was unexpected because rats are known to steadily decrease their exploration of extended open fields presumably due to growing familiarity. Moreover, this evidence of learning results in still greater decreases in exploration on following days, an effect indicative of long-term memory. We concluded that the apparatus was too complicated to be mastered in the allotted test periods. Further work then showed that several days of experience with complexity enabled

rapid and persistent memory encoding in the novel situation. Humans deal with new and challenging circumstances by transferring rules acquired during their past encounters with related, though clearly different circumstances (Baldwin et al., 1988; Pan et al., 2010). Our studies appear to have uncovered a first instance of this in rodents. Rats with prior experience with complexity altered the timing and structure of their exploratory episodes, in ways that appear to have promoted more effective encoding, and led to unexpectedly discrete synaptic changes in the output stage of hippocampus (see below). We think that this is an important development that will open the way to the first neurobiological studies of a critical aspect of human episodic memory. Beyond this, the results describe a paradigm for the above noted analyses of rodent hippocampus during behavior that involves what', 'where', and 'when' during discrete instances of episodic exploration. We intend to exploit this opportunity in future work using the transient silencing procedure noted above.

The present thesis work used this behavioral paradigm to localize sites in hippocampus in which learning produced the greatest concentration of synapses associated with a marker for LTP. The results were unexpected in that such effects were predominantly found in an area, involving both basal and proximal apical dendrites, centered on field CA1b. This area constitutes the final step of intra-hippocampal circuitry and we assume that it serves to integrate the three episodic memory elements processed at earlier stages. If this is correct, then the most intense memory related synaptic changes are likely related to building a unitary code for the information collected during a sequence of forays. It is interesting in this regard that in addition to records of items, spatial relations, and time, episodic memories are likely to have some type of code that distinguishes them from each other. This follows from the commonplace experience of first locating an episode and then reading its contents. Operations of this type would be far more efficient if some type of marker could be used to identify the stored sequences, which must be present in enormous numbers in humans. Relatedly, psychological studies show that retrieved episodes can be linked together into novel arrangements, a process argued to be

critical to inferential thinking (Zeithamova et al., 2012). Such effects would again be easier to achieve if episodes could be treated as units by the cortex. But how would rodents with their poorly developed cortical association fields make use of a tagging mechanism for a complex series of experiences? One possibility is that it provides a recognition signal for a thoroughly explored environment, something likely to be vital for survival. Re-experiencing the environment during an initial foray on the day after the first exploration would, by this account, activate a very strong output from hippocampus that would depend, for reactivation, on the presence of the same cues and spatio-temporal relationships found on the previous day. Changes between days in any of these complex associations would result in firing by cells that had not been linked via LTP to field CA1 and thus the possibility of an error signal. In essence, the timing device provided by the dentate gyrus-CA3 subsystem, together with encoded information about cues and their relative locations, would constitute a system that can detect even subtle alterations to an environment.

This above work also includes the development of several technologies with potentially broad application. The model of the CA3, if it can be generalized into an algorithm, would constitute a novel approach to using a network to store and process episodic information. This would allow for systems which could receive and organize complex information spaced at human relevant scales. As this system maintains and organizes temporal information into spatial information, it is highly applicable to neural network technologies. The mapping technology developed here has broad applications to the search for an engram (Lashley, 1950). It can be used to map the activation patterns of synapses in any region that has been identified as a candidate for memory storage. The technology has to be advanced further to allow individual differences in storage sites to be identified. Also further studies must explore the exact scale of these ‘hot spots’ of storage. The mapping combined with the modeling also allows development of more explicit models that might predict novel network architecture which would further increase the power of developed algorithms.

In summary, our modeling, physiological, and behavioral studies point to the conclusion that the highly specialized and evolutionarily conserved characteristics of hippocampus generate unique time related computations. These effects are essential for dealing with the complexity of real world environments by most, and perhaps all, groups of mammals. But the results go beyond this to describe emergent properties of the networks that help explain the origins of salient features of human episodic memory.

# References


Abraham, W. C., Logan, B., Greenwood, J. M., & Dragunow, M. (2002). Induction and experience-dependent consolidation of stable long-term potentiation lasting months in the hippocampus. *J Neurosci*, *22*(21), 9626–9634. https://doi.org/22/21/9626 [pii]

Amaral, D. G., Ishizuka, N., & Claiborne, B. (1990). Chapter 1 Chapter Neurons, numbers and the hippocampal network (pp. 1–11). https://doi.org/10.1016/S0079-6123(08)61237-6

Amaral, D. G., Scharfman, H. E., & Lavenex, P. (2007). The dentate gyrus: fundamental neuroanatomical organization (dentate gyrus for dummies). *Progress in Brain Research*, *163*, 3–22. https://doi.org/10.1016/S0079-6123(07)63001-5

Ambros-Ingerson, J., Granger, R., & Lynch, G. (1990). Simulation of paleocortex performs hierarchical clustering. *Science*, *247*(4948). Retrieved from http://science.sciencemag.org/content/247/4948/1344

Amit, D. J. (1995). The Hebbian paradigm reintegrated: Local reverberations as internal representations. *Behavioral and Brain Sciences*, *18*(4), 617. https://doi.org/10.1017/S0140525X00040164

Baldwin, T. T. ., & Ford, J. K. (1988). Transfer of Training: a Review and Directions for Future Research. *Personnel Psychology*, *41*(1), 63–105. https://doi.org/10.1111/j.1744-6570.1988.tb00632.x

Baudry, M., Bi, X., Gall, C., & Lynch, G. (2011). The biochemistry of memory: The 26year journey of a “new and specific hypothesis”. *Neurobiology of Learning and Memory*, *95*(2), 125–133. https://doi.org/10.1016/j.nlm.2010.11.015

Bienenstock, E., Cooper, L., & Munro, P. (1982). Theory for the development of neuron selectivity: orientation specificity and binocular interaction in visual cortex. *Journal of Neuroscience*, *2*(1). Retrieved from http://www.jneurosci.org/content/2/1/32.long

Bliss, T. V. P., & Collingridge, G. L. (1993). A synaptic model of memory: long-term potentiation in the hippocampus. *Nature*, *361*(6407), 31–39. https://doi.org/10.1038/361031a0

Bota, M., Sporns, O., & Swanson, L. W. (2015). Architecture of the cerebral cortical association connectome underlying cognition. *Proceedings of the National Academy of Sciences of the United States of America*, *112*(16), E2093-101. https://doi.org/10.1073/pnas.1504394112

Buzsáki, G. (1986). Hippocampal sharp waves: their origin and significance. *Brain Research*, *398*(2), 242–52. Retrieved from http://www.ncbi.nlm.nih.gov/pubmed/3026567

Canto, C. B., Wouterlood, F. G., & Witter, M. P. (2008). What does the anatomical organization of the entorhinal cortex tell us? *Neural Plasticity*, *2008*, 381243.

https://doi.org/10.1155/2008/381243

Chapuis, J., Cohen, Y., He, X., Zhang, Z., Jin, S., Xu, F., & Wilson, D. A. (2013). Lateral Entorhinal Modulation of Piriform Cortical Activity and Fine Odor Discrimination. *Journal of Neuroscience*, *33*(33), 13449–13459. https://doi.org/10.1523/JNEUROSCI.1387-13.2013

Chen, L. Y., Rex, C. S., Casale, M. S., Gall, C. M., & Lynch, G. (2007). Changes in synaptic morphology accompany actin signaling during LTP. *The Journal of Neuroscience : The Official Journal of the Society for Neuroscience*, *27*(20), 5363–72. https://doi.org/10.1523/JNEUROSCI.0164-07.2007

Chen, X., Guo, Y., Feng, J., Liao, Z., Li, X., Wang, H., … He, J. (2013). Encoding and Retrieval of Artificial Visuoauditory Memory Traces in the Auditory Cortex Requires the Entorhinal Cortex. *Journal of Neuroscience*, *33*(24). Retrieved from http://www.jneurosci.org/content/33/24/9963

Clayton, N. S., & Dickinson, A. (1998). Episodic-like memory during cache recovery by scrub jays. *Nature*, *395*(6699), 272–274. https://doi.org/10.1038/26216

Clayton, N. S., Griffiths, D. P., Emery, N. J., & Dickinson, A. (2001). Elements of episodic–like memory in animals. *Philosophical Transactions of the Royal Society of London B: Biological Sciences*, *356*(1413). Retrieved from http://rstb.royalsocietypublishing.org/content/356/1413/1483?ijkey=1369ef7de4ef01d3f1c7e6b4218dc0611f8fd9c3&keytype2=tf_ipsecsha

Compte, A., Brunel, N., Goldman-Rakic, P. S., & Wang, X.-J. (2000). Synaptic Mechanisms and Network Dynamics Underlying Spatial Working Memory in a Cortical Network Model. *Cerebral Cortex*, *10*(9), 910–923. https://doi.org/10.1093/cercor/10.9.910

Coultrip, R., Granger, R., & Lynch, G. (1992). A cortical model of winner-take-all competition via lateral inhibition.

Deadwyler, S. A., Gribkoff, V., Cotman, C., & Lynch, G. (1976). Long lasting changes in the spontaneous activity of hippocampal neurons following stimulation of the entorhinal cortex. *Brain Research Bulletin*, *1*(1), 1–7. https://doi.org/10.1016/0361-9230(76)90043-5

Deadwyler, S. A., West, J. R., Cotman, C. W., & Lynch, G. S. (1975). A neurophysiological analysis of commissural projections to dentate gyrus of the rat. *Journal of Neurophysiology*, *38*(1), 167–184. Retrieved from http://jn.physiology.org/content/38/1/167.long

Deadwyler, S. A., West, M., & Lynch, G. (1979). Synaptically identified hippocampal slow potentials during behavior. *Brain Research*, *161*(2), 211–225. https://doi.org/10.1016/0006-8993(79)90064-7

Dede, A. J. O., Frascino, J. C., Wixted, J. T., & Squire, L. R. (2016). Learning and remembering

real-world events after medial temporal lobe damage. *Proceedings of the National Academy of Sciences*, 1–6. https://doi.org/10.1073/pnas.1617025113

Dunwiddie, T., & Lynch, G. (1978). Long-term potentiation and depression of synaptic responses in the rat hippocampus: localization and frequency dependency. *The Journal of Physiology*, *276*, 353–67. Retrieved from http://www.ncbi.nlm.nih.gov/pubmed/650459

Easton, A., Webster, L. A. D., & Eacott, M. J. (2012). The episodic nature of episodic-like memories. *Learning & Memory (Cold Spring Harbor, N.Y.)*, *19*(4), 146–50. https://doi.org/10.1101/lm.025676.112

Eichenbaum, H. (2014). Time cells in the hippocampus: a new dimension for mapping memories. *Nature Reviews. Neuroscience*, *15*(11), 732–44. https://doi.org/10.1038/nrn3827

Eichenbaum, H., Sauvage, M., Fortin, N., Komorowski, R., & Lipton, P. (2012, August). Towards a functional organization of episodic memory in the medial temporal lobe. *Neuroscience and Biobehavioral Reviews*. NIH Public Access. https://doi.org/10.1016/j.neubiorev.2011.07.006

Eilam, D., & Golani, I. (1989). Home base behavior of rats (Rattus norvegicus) exploring a novel environment. *Behavioural Brain Research*, *34*(3), 199–211. Retrieved from http://www.ncbi.nlm.nih.gov/pubmed/2789700

Farovik, A., Dupont, L. M., & Eichenbaum, H. (2010). Distinct roles for dorsal CA3 and CA1 in memory for sequential nonspatial events. *Learning & Memory (Cold Spring Harbor, N.Y.)*, *17*(1), 12–17. https://doi.org/10.1101/lm.1616209

Globus, A., Rosenzweig, M. R., Bennett, E. L., & Diamond, M. C. (1973). Effects of differential experience on dendritic spine counts in rat cerebral cortex. *Journal of Comparative and Physiological Psychology*, *82*(2), 175–81. Retrieved from http://www.ncbi.nlm.nih.gov/pubmed/4571892

Granger, R., Whitson, J., Larson, J., Lynch, G., & Thompson, R. F. (1994). Non-Hebbian properties of long-term potentiation enable high-capacity encoding of temporal sequences (non-Hebbian Iearnlng/hippocampus/long-term potentiation learning rules). *Neurobiology*, *91*, 10104–10108. Retrieved from http://www.pnas.org/content/91/21/10104.long

Greenough, W. T., Volkmar, F. R., & Juraska, J. M. (1973). Effects of rearing complexity on dendritic branching in frontolateral and temporal cortex of the rat. *Experimental Neurology*, *41*(2), 371–8. https://doi.org/10.1016/0014-4886(73)90278-1

Gunn, B. G., Cox, C. D., Chen, Y., Frotscher, M., Gall, C. M., Baram, T. Z., & Lynch, G. (2017). The Endogenous Stress Hormone CRH Modulates Excitatory Transmission and Network

Physiology in Hippocampus. *Cerebral Cortex*, 1–17. https://doi.org/10.1093/cercor/bhx103

Guzman, S. J., Schlögl, A., Frotscher, M., & Jonas, P. (2016). Synaptic mechanisms of pattern completion in the hippocampal CA3 network. *Science*, *353*(6304). Retrieved from http://science.sciencemag.org/content/353/6304/1117.full

Hafting, T., Fyhn, M., Molden, S., Moser, M. B., & Moser, E. I. (2005). Microstructure of a spatial map in the entorhinal cortex. *Nature*, *436*(7052), 801–806. https://doi.org/nature03721 [pii] 10.1038/nature03721

Hajos, N., Karlocai, M. R., Nemeth, B., Ulbert, I., Monyer, H., Szabo, G., … Gulyas, A. I. (2013). Input-Output Features of Anatomically Identified CA3 Neurons during Hippocampal Sharp Wave/Ripple Oscillation In Vitro. *Journal of Neuroscience*, *33*(28), 11677–11691. https://doi.org/10.1523/JNEUROSCI.5729-12.2013

Hall, C., & Ballachey, E. L. (1932). A study of the rat's behavior in a field. A contribution to method in comparative psychology. *University of California Publications in Psychology*. Retrieved from http://psycnet.apa.org/psycinfo/1932-04321-001

Hargreaves, E. L., Rao, G., Lee, I., & Knierim, J. J. (2005). Major Dissociation Between Medial and Lateral Entorhinal Input to Dorsal Hippocampus. *Science*, *308*(5729). Retrieved from http://science.sciencemag.org/content/308/5729/1792.long

Harris, K. M., Jensen, F. E., & Tsao, B. (1992). Three-dimensional structure of dendritic spines and synapses in rat hippocampus (CA1) at postnatal day 15 and adult ages: implications for the maturation of synaptic physiology and long-term potentiation. *The Journal of Neuroscience : The Official Journal of the Society for Neuroscience*, *12*(7), 2685–705. Retrieved from http://www.ncbi.nlm.nih.gov/pubmed/1613552

Hasselmo, M. E., & Stern, C. E. (2006). Mechanisms underlying working memory for novel information. *Trends in Cognitive Sciences*, *10*(11), 487–493. https://doi.org/10.1016/j.tics.2006.09.005

Hopfield, J. J. (1982). Neural networks and physical systems with emergent collective computational abilities (associative memory/parallel processing/categorization/content-addressable memory/fail-soft devices). *Biophysics*, *79*, 2554–2558. Retrieved from http://www.pnas.org/content/79/8/2554.full.pdf

Jarsky, T., Roxin, A., Kath, W. L., & Spruston, N. (2005). Conditional dendritic spike propagation following distal synaptic activation of hippocampal CA1 pyramidal neurons. *Nature Neuroscience*, *8*(12), 1667–1676. https://doi.org/10.1038/nn1599

Jochems, A., Reboreda, A., Hasselmo, M. E., & Yoshida, M. (2013). Cholinergic receptor activation supports persistent firing in layer III neurons in the medial entorhinal cortex.

*Behavioural Brain Research*, *254*, 108–115. https://doi.org/10.1016/j.bbr.2013.06.027

Kesner, R. P., & Rolls, E. T. (2015). A computational theory of hippocampal function, and tests of the theory: New developments. *Neuroscience & Biobehavioral Reviews*, *48*, 92–147. https://doi.org/10.1016/j.neubiorev.2014.11.009

Kubota, D., Colgin, L. L., Casale, M., Brucher, F. A., & Lynch, G. (2002). Endogenous Waves in Hippocampal Slices. *Journal of Neurophysiology*, *89*(1), 81–89. https://doi.org/10.1152/jn.00542.2002

Lashley, K. (1950). In search of the engram. *Symposia of the Society for Experimental …*. Retrieved from http://psychology.stanford.edu/~jlm/pdfs/Lashley50Engram.pdf

Leggio, M. G., Mandolesi, L., Federico, F., Spirito, F., Ricci, B., Gelfo, F., & Petrosini, L. (2005). Environmental enrichment promotes improved spatial abilities and enhanced dendritic growth in the rat. *Behavioural Brain Research*, *163*(1), 78–90. https://doi.org/10.1016/j.bbr.2005.04.009

Lynch, G., & Baudry, M. (1984). The biochemistry of memory: a new and specific hypothesis. *Science*, *224*(4653). Retrieved from http://science.sciencemag.org/content/224/4653/1057.long

MacDonald, C. J., Lepage, K. Q., Eden, U. T., & Eichenbaum, H. (2011). Hippocampal "time cells" bridge the gap in memory for discontiguous events. *Neuron*, *71*(4), 737–49. https://doi.org/10.1016/j.neuron.2011.07.012

Maier, N., Nimmrich, V., & Draguhn, A. (2003). Cellular and Network Mechanisms Underlying Spontaneous Sharp Wave-Ripple Complexes in Mouse Hippocampal Slices. *The Journal of Physiology*, *550*(3), 873–887. https://doi.org/10.1113/jphysiol.2003.044602

Marr, D. (1971). Simple Memory: A Theory for Archicortex. *Philosophical Transactions of the Royal Society of London B: Biological Sciences*, *262*(841). Retrieved from http://rstb.royalsocietypublishing.org/content/262/841/23.long

McEchron, M. D., Tseng, W., & Disterhoft, J. F. (2003). Single neurons in CA1 hippocampus encode trace interval duration during trace heart rate (fear) conditioning in rabbit. *The Journal of Neuroscience : The Official Journal of the Society for Neuroscience*, *23*(4), 1535–47. Retrieved from http://www.ncbi.nlm.nih.gov/pubmed/12598642

Migliore, M., Morse, T. M., Davison, A. P., Marenco, L., Shepherd, G. M., & Hines, M. L. (2003). ModelDB: Making Models Publicly Accessible to Support Computational Neuroscience. *Neuroinformatics*, *1*(1), 135–140. https://doi.org/10.1385/NI:1:1:135

Miles, R., & Wong, R. K. (1986). Excitatory synaptic interactions between CA3 neurones in the guinea-pig hippocampus. *The Journal of Physiology*, *373*, 397–418. Retrieved from

http://www.ncbi.nlm.nih.gov/pubmed/3018233

Modi, M. N., Dhawale, A. K., & Bhalla, U. S. (2014). CA1 cell activity sequences emerge after reorganization of network correlation structure during associative learning. *eLife*, *2014*(3), e01982–e01982. https://doi.org/10.7554/eLife.01982

Nádasdy, Z., Hirase, H., Czurkó, A., Csicsvari, J., & Buzsáki, G. (1999). Replay and Time Compression of Recurring Spike Sequences in the Hippocampus. *Journal of Neuroscience*, *19*(21). Retrieved from http://www.jneurosci.org/content/19/21/9497.short

Nicholson, D. A., Trana, R., Katz, Y., Kath, W. L., Spruston, N., & Geinisman, Y. (2006). Distance-Dependent Differences in Synapse Number and AMPA Receptor Expression in Hippocampal CA1 Pyramidal Neurons. *Neuron*, *50*(3), 431–442. https://doi.org/10.1016/j.neuron.2006.03.022

Norman, K. A., & O'Reilly, R. C. (2003). Modeling hippocampal and neocortical contributions to recognition memory: A complementary-learning-systems approach. *Psychological Review*, *110*(4), 611–646. https://doi.org/10.1037/0033-295X.110.4.611

Oh, S. W., Harris, J. A., Ng, L., Winslow, B., Cain, N., Mihalas, S., … Zeng, H. (2014). A mesoscale connectome of the mouse brain. *Nature*, *508*(7495), 207–14. https://doi.org/10.1038/nature13186

Pan, S. J., & Yang, Q. (2010). A Survey on Transfer Learning. *IEEE Transactions on Knowledge and Data Engineering*, *22*(10), 1345–1359. https://doi.org/10.1109/TKDE.2009.191

Petersen, J. D., Chen, X., Vinade, L., Dosemeci, A., Lisman, J. E., & Reese, T. S. (2003). Distribution of postsynaptic density (PSD)-95 and Ca2+/calmodulin-dependent protein kinase II at the PSD. *The Journal of Neuroscience : The Official Journal of the Society for Neuroscience*, *23*(35), 11270–8. Retrieved from http://www.ncbi.nlm.nih.gov/pubmed/14657186

Pinsky, P. F., & Rinzel, J. (1994). Intrinsic and network rhythmogenesis in a reduced Traub model for CA3 neurons. *Journal of Computational Neuroscience*, *1*(1–2), 39–60. Retrieved from http://www.ncbi.nlm.nih.gov/pubmed/8792224

Rebola, N., Carta, M., & Mulle, C. (2017). Operation and plasticity of hippocampal CA3 circuits: implications for memory encoding. *Nature Publishing Group*, *18*. https://doi.org/10.1038/nrn.2017.10

Rex, C. S., Chen, L. Y., Sharma, A., Liu, J., Babayan, A. H., Gall, C. M., & Lynch, G. (2009). Different Rho GTPase-dependent signaling pathways initiate sequential steps in the consolidation of long-term potentiation. *J Cell Biol*, *186*(1), 85–97.

https://doi.org/jcb.200901084 [pii] 10.1083/jcb.200901084

Rex, C. S., Colgin, L. L., Jia, Y., Casale, M., Yanagihara, T. K., Debenedetti, M., … Lynch, G. (2009). Origins of an intrinsic hippocampal EEG pattern. *PLoS ONE*, *4*(11), e7761. https://doi.org/10.1371/journal.pone.0007761

Rolls, E. T. (2008). Computational Models of Hippocampal Functions. In *Learning and Memory: A Comprehensive Reference* (pp. 641–666). https://doi.org/10.1016/B978-0-12-809324-5.21025-0

Roth, L. R., & Stan Leung, L. (1995). Difference in LTP at basal and apical dendrites of CA1 pyramidal neurons in urethane-anesthetized rats. *Brain Research*, *694*(1), 40–48. https://doi.org/10.1016/0006-8993(95)00767-K

Salz, D. M., Tiganj, Z., Khasnabish, S., Kohley, A., Sheehan, D., Howard, M. W., & Eichenbaum, H. (2016). Time Cells in Hippocampal Area CA3. *Journal of Neuroscience*, *36*(28). Retrieved from http://www.jneurosci.org/content/36/28/7476

Sassoé-Pognetto, M., Utvik, J. K., Camoletto, P., Watanabe, M., Stephenson, F. A., Bredt, D. S., & Ottersen, O. P. (2003). Organization of postsynaptic density proteins and glutamate receptors in axodendritic and dendrodendritic synapses of the rat olfactory bulb. *Journal of Comparative Neurology*, *463*(3), 237–248. https://doi.org/10.1002/cne.10745

Schlingloff, D., Kali, S., Freund, T. F., Hajos, N., & Gulyas, A. I. (2014). Mechanisms of Sharp Wave Initiation and Ripple Generation. *Journal of Neuroscience*, *34*(34), 11385–11398. https://doi.org/10.1523/JNEUROSCI.0867-14.2014

Seltzer, B., & Pandya, D. N. (1976). Some cortical projections to the parahippocampal area in the rhesus monkey. *Experimental Neurology*, *50*(1), 146–160. https://doi.org/10.1016/0014-4886(76)90242-9

Smith, M. A., Ellis-Davies, G. C., & Magee, J. C. (2003). Mechanism of the distance-dependent scaling of Schaffer collateral synapses in rat CA1 pyramidal neurons. *J Physiol*, *548*(Pt 1), 245–258. https://doi.org/10.1113/jphysiol.2002.036376 2002.036376 [pii]

Squire, L. R., Stark, C. E. L., & Clark, R. E. (2004). THE MEDIAL TEMPORAL LOBE. *Annual Review of Neuroscience*, *27*(1), 279–306. https://doi.org/10.1146/annurev.neuro.27.070203.144130

Striedter, G. F. (2016). Evolution of the hippocampus in reptiles and birds. *Journal of Comparative Neurology*, *524*(3), 496–517. https://doi.org/10.1002/cne.23803

Taxidis, J., Coombes, S., Mason, R., & Owen, M. R. (2012). Modeling sharp wave-ripple complexes through a CA3-CA1 network model with chemical synapses. *Hippocampus*, *22*(5), 995–1017. https://doi.org/10.1002/hipo.20930

Treves, A., & Rolls, E. T. (1994). Computational analysis of the role of the hippocampus in memory. *Hippocampus*, *4*(3), 374–391. https://doi.org/10.1002/hipo.450040319

Trieu, B. H., Kramár, E. A., Cox, C. D., Jia, Y., Wang, W., Gall, C. M., & Lynch, G. (2015). Pronounced differences in signal processing and synaptic plasticity between piriform-hippocampal network stages: a prominent role for adenosine. *The Journal of Physiology*, *593*(13), 2889–2907. https://doi.org/10.1113/JP270398

Tse, D., Takeuchi, T., Kakeyama, M., Kajii, Y., Okuno, H., Tohyama, C., … Morris, R. G. M. (2011). Schema-dependent gene activation and memory encoding in neocortex. *Science*, *333*(6044), 891–895. https://doi.org/science.1205274 [pii] 10.1126/science.1205274

Tulving, E. (1985). *Elements of episodic memory*. Clarendon. Retrieved from https://global.oup.com/academic/product/elements-of-episodic-memory-9780198521259?cc=us&lang=en&

Tulving, E., Schacter, D. L., McLachlan, D. R., & Moscovitch, M. (1988). Priming of semantic autobiographical knowledge: a case study of retrograde amnesia. *Brain and Cognition*, *8*(1), 3–20. Retrieved from http://www.ncbi.nlm.nih.gov/pubmed/3166816

Urban, N. N., Henze, D. A., & Barrionuevo, G. (2001). Revisiting the role of the hippocampal mossy fiber synapse. *Hippocampus*, *11*(4), 408–417. https://doi.org/10.1002/hipo.1055

Valtschanoff, J. G., & Weinberg, R. J. (2001). Laminar organization of the NMDA receptor complex within the postsynaptic density. *The Journal of Neuroscience : The Official Journal of the Society for Neuroscience*, *21*(4), 1211–7. Retrieved from http://www.ncbi.nlm.nih.gov/pubmed/11160391

van Praag, H., Kempermann, G., & Gage, F. H. (2000). Neural consequences of environmental enrichment. *Nature Reviews Neuroscience*, *1*(3), 191–198.

van Strien, N. M., Cappaert, N. L. M., & Witter, M. P. (2009). The anatomy of memory: an interactive overview of the parahippocampal–hippocampal network. *Nature Reviews Neuroscience*, *10*(4), 272–282. https://doi.org/10.1038/nrn2614

Vogels, T. P., Rajan, K., & Abbott, L. F. (2005). Neural Network Dynamics. https://doi.org/10.1146/

Wallenstein, G. V., Eichenbaum, H., Hasselmo, M. E., & Eichenbaum, H. The hippocampus as an associator of discontiguous events, 21 Trends in Neurosciences § (1998). https://doi.org/10.1016/S0166-2236(97)01220-4

Walsh, R. N., & Cummins, R. A. (1976). The Open-Field Test: a critical review. *Psychological Bulletin*, *83*(3), 482–504. Retrieved from http://www.ncbi.nlm.nih.gov/pubmed/17582919

Wang, W., Trieu, B. H., Palmer, L. C., Jia, Y., Pham, D. T., Jung, K.-M., … Lynch, G. (2016). A

Primary Cortical Input to Hippocampus Expresses a Pathway-Specific and Endocannabinoid-Dependent Form of Long-Term Potentiation. *eNeuro*, *3*(4), 160–16. https://doi.org/10.1523/ENEURO.0160-16.2016

Wang, X. J., & Buzsáki, G. (1996). Gamma oscillation by synaptic inhibition in a hippocampal interneuronal network model. *The Journal of Neuroscience : The Official Journal of the Society for Neuroscience*, *16*(20), 6402–13. Retrieved from http://www.ncbi.nlm.nih.gov/pubmed/8815919

Wilson, D. I. G., Langston, R. F., Schlesiger, M. I., Wagner, M., Watanabe, S., & Ainge, J. A. (2013). Lateral entorhinal cortex is critical for novel object-context recognition. *Hippocampus*, *23*(5), 352–66. https://doi.org/10.1002/hipo.22095

Zeithamova, D., Dominick, A. L., & Preston, A. R. (2012). Hippocampal and Ventral Medial Prefrontal Activation during Retrieval-Mediated Learning Supports Novel Inference. *Neuron*, *75*(1), 168–179. https://doi.org/10.1016/j.neuron.2012.05.010